The role of LTN1 in dMMR CRC cancer

MSc(Res) Oncology, 2024

Eleanor Smith

Contents

Abbreviations....3
Abstract....5
Introduction....7
T cells in cancer....9
Mechanism of microsatellite instability....11
Mechanisms of antigen presentation....15
The ubiquitin-proteasome system....17
Ribosomal Quality Control....18
The importance of LTN1....22
The structure of LTN1....24
RQC generates neoantigens....25
Materials and Methods....26
Cell Culture....26
Flow Cytometry....27
Protein preparations and western blot analysis....28
Transient transfection for protein expression....29
Polymerase chain reaction....30
Agarose gel electrophoresis....31
Sanger sequencing....31
Nucleic acid quantification....32
RNA, cDNA synthesis and qRT-PCR....32
Plasmid constructs....33
Bacterial transformation....34
Mini-prep plasmid extraction....35
Generation of the LTN1WT and LTN1ΔRING HCT116 stable expressing cell lines....35
Determining Blasticidin sensitivity of lentiviral transduced HCT116 cells....36
Results....36
The HCT116 MSI cells are a naturally occurring knockout of the LTN1 protein....36
MRNA expression levels of LTN1 in HCT116 cells....41
Transient LTN1 expression in HCT116 upregulates MHC-I expression....42
Generation of a LTN1 RING deletion mutant....45
Discussion....53
Concluding remarks....62
Acknowledgements....63
Bibliography....64
Supplementary material....80

Abbreviations

ATP – Adenosine Triphosphate

APM – Antigen presentation machinery

β2M – β2-microglobulin

CAT – C-terminal addition to translation

CD – Cluster of differentiation

CRC – Colorectal carcinoma

CTLA4 – Cytotoxic T-lymphocyte associated protein 4

DNA – Deoxyribonucleic acid

DRiP – defective ribosomal product

ER – endoplasmic reticulum

ELISpot – enzyme-linked immunosorbent spot

FSP – frameshift peptides

FOX-P3 – forkhead box protein 3

HECT – E6-AP Carboxyl Terminus

HLA – human leukocyte antigen

HNPCC – Hereditary nonpolyposis colon cancer

IL – Interleukin

INDEL – Insertion/deletion

KIR – killer cell immunoglobulin-like receptor

LTN1 – listerin E3 ubiquitin protein ligase 1

MAIT cells – mucosal associated invariant T cells

MMR – Mismatch repair

dMMR – MMR deficiency

MLH1 – DNA mismatch repair protein Mlh1

MSI – Microsatellite instability

MSI-H –MSI high

MSI-L – MSI low

MSH – MutS Homolog

MSS – micro satellite stable

NEMF – nuclease export mediator factor

NFAT – nuclear factor of activated T cells

NF-κB – Nuclear factor kappa-light-chain-enhancer of activated B cells

NHS – UK National Health Service

NK cells – natural killer cells

NMD – Nonsense-mediated mRNA decay

iNKT cells – invariant natural killer T cells

PCNA – Proliferating cell nuclear antigen

PCR – polymerase chain reaction

PD-1 – Programmed cell death protein 1

PD-L1 – Programmed death-ligand 1

PMS2 – Mismatch repair endonuclease PMS2

RBR – Ring-Between-Ring

RAS – Rat sarcoma virus

RING – Really Interesting New Gene

RPM – rotations per minute

RNA – Ribonucleic acid

RQC – ribosomal quality control

RT-qPCR – Real time quantitative PCR

SHP2 – Src homology region 2-containing protein tyrosine phosphatase 2

UPS – ubiquitin-proteasome system

TAP – Transporter for antigen presentation

TCR – T cell antigen receptor

TGF – Transforming growth factor

TNF-α – Tumour Necrosis Factor alpha

Treg – T regulatory

VCP– valosin-containing protein

WPRE – Woodchuck Hepatitis Virus Posttranscriptional Regulatory Element

ZAP70 – Zeta-chain-associated protein kinase 70

ZNF598 – Zinc Finger Protein 598

Abstract

The intracellular proteome of mammalian cells is monitored through the presentation of peptides bound to major histocompatibility (MHC) class I molecules on the surface of all nucleated cells. The adaptive immune system is primed to recognise these peptides, identifying and eliminating cells that present anything aberrant. The oncogenic transformation of a cell requires the alteration of a cell's genome, modulating its proteome in a way that promotes tumour development. Such proteins, when presented, are recognised as foreign, leaving the tumour susceptible to immune-mediated destruction. As a consequence of this immune pressure, tumour cells employ several evasion strategies to hide their proteome from the immune system. This most commonly manifests in the mutation of genes involved in antigen presentation, such as MHC class I, β2-microglobulin, and the transporter associated with antigen processing (TAP). The present study aims to investigate whether mutations at an earlier stage in antigen presentation serve to evade the immune system in a more specific manner. LTN1 is an E3 ubiquitin ligase with a central role in the degradation of mutant proteins, and has recently been found to directly control the presentation of specific peptides. Importantly, frequent loss of function mutations in LTN1 have been identified in microsatellite instability high (MSI-H) CRCs.

We hypothesize that colorectal carcinomas (CRCs) mutate LTN1 to prevent the presentation of neoantigens, and thus evade immune detection. We believe that the frameshift mutant LTN1 can serve itself as a neoantigen and may be an important target for the development of frameshift derived vaccines. Here we establish a biologically relevant model for the study of LTN1 in antigen presentation, and find that rescuing LTN1 loss of function increases total antigen presentation. Furthermore, we establish the foundation for future immunopeptidomic analysis to reveal the specific peptides LTN1 targets in human CRC.

Introduction

Globally, cancer is one of the most common and challenging diseases, witnessing approximately 18 million newly diagnosed cases during 2020[1], and whilst significant progress has been made in cancer research and treatment, there is still a pressing need for more effective therapies across various types of cancers. From the seminal observation that cancer arises as a consequence of DNA mutations[2], the field has made significant advancements in determining the necessary changes for the transformation of a cell into a malignant tumour. Hanahan and Weinberg defined these characteristics as the 'hallmarks of cancer', a conceptual framework that has since been further elaborated and extensively documented[3]. The acquisition of these hallmarks necessitates a cell's ability to subvert programmed cell death, sustain proliferative signalling, evade growth suppressors, enable replicative immortality, induce angiogenesis, invade nearby tissues and metastasize to distant parts of the body[3]. These hallmark characteristics collectively converge on the fundamental concept of genomic instability, a phenomenon subsequently recognized by Hanahan and Weinberg as an emerging hallmark in the development of cancer[4]. Genomic instability allows the accumulation of mutations within a cell's genome, a subset of which confers selective advantages, culminating in the acquisition of all the aforementioned hallmark traits[4].

In order to report cellular ongoings, all nucleated cells present a selection of intracellular-derived peptides on their cell surface, originating from the cell's own proteome[5], and the repertoire of peptides presented is referred to as a cell's immunopeptidome[6]. Such peptides are presented on major histocompatibility complex class I (MHC-I) molecules and the complex of peptide-bound MHC is recognised by CD8+ cytotoxic T cells of the immune system[7].

Antigen recognition by T cells occurs by the surface bound T cell receptor antigen (TCR), a specialised adaptive immune protein[8]. These proteins are highly diverse in sequence in order to detect the wide range of peptide antigens that could be presented on the surface of a cell by MHC molecules[9]. The TCR discriminates 'self'-peptides from non-'self', with the latter priming the T cell to eliminate the problematic cell[10]. In order to generate the necessary diversity of TCRs, T cells undergo a stochastic rearrangement of their TCR gene locus, known as V(D)J recombination[11]. These molecules are heterodimers, mainly formed of an α- and β-chain, however a small percentage instead express a γ- and δ-chain[11]. To ensure each newly generated TCR sequence is able to recognise peptide bound MHC, but does not recognise 'self'-peptides, each newly formed TCR must undergo thymic selection[12]. This commences with positive selection whereby the TCR binds to cortical thymic epithelial cells expressing 'self'-peptide bound to MHC to ensure the TCR is functional[13]. T cells are defined by the expression of the co-receptor molecules CD4 and CD8[10]. A thymocyte will initially express neither co-receptor, but whilst selection ensues, a T cell will commit to either the CD4+ or CD8+ lineage, and this process is initiated during positive selection[14]. Thymocytes are subsequently negatively selected in the thymic medulla whereby they are removed if they bind too strongly to 'self'-pMHC (termed clonal deletion), thus ensuring the TCR will not initiate an autoimmune response[12]. At this stage further differences in TCR signalling can result in changes to the characteristics of the T cell. Strong TCR engagement during thymocyte development that is below the threshold required for negative selection can result in the differentiation of thymocytes into T regulatory cells (Treg)[15, 16, 17]. Tregs are an example of one subset of a polarised T cell, defined by their expression of the forkhead box protein P3 (FOX-P3) transcription factor, which results in a varying cytokine profile compared to conventional T cells[18]. The completion of thymic selection ensures mature T cells exhibit functional, non-'self'-reactive TCRs[19]. These T cells are predominantly

committed to either CD8+ cytotoxic or CD4+ helper lineages[10], with a smaller fraction committed to minor subsets such as Treg, invariant natural killer T cells (iNKT cells), or mucosal associated invariant T cells (MAIT cells)[20]. Lineage commitment defines the effector function of each T cell subset, arming the immune system with an array of specialised responses[20].

T cells in cancer

Tumour cells are no exception to T cell-mediated immune surveillance and as a cell undergoes malignant transformation, the presentation of its antigens continues[21]. Consequently, peptides derived from tumorigenic proteins may be presented on the cell surface[21]. As these peptides derive from mutant DNA, they would not have been eliminated during negative selection and therefore have the potential to be recognised by T cells[21]. During the lifetime of an individual, such oncogenic changes may occur, but these can be detected and killed by the immune system[21]. For a successful tumour to develop it must escape immune-mediated killing, and this process is referred to as immunoediting[21]. Successful immune evasion can take a variety of forms, the specificities of which dependent on the particular tumour[21].

One mechanism by which a tumour can escape immune scrutiny is through fostering an immunosuppressive microenvironment[22]. A tumour microenvironment can contain different T cell subsets which will have varying roles in tumourigenesis[22]. Whilst CD8+ T cells may have an anti-tumour effect through the direct recognition and killing of tumour cells, Treg cells have the opposite effect and are pro-tumorigenic[22]. The balance between pro- and anti-tumorigenic T cells has been shown to be a determinant of tumour progression, with high numbers of Treg cells being associated with a reduced overall patient survival in a variety of

different cancers[23]. Treg cells exert their immunosuppression through a variety of mechanisms: consumption and therefore competition of IL-2 which is necessary for conventional T cell activation[24, 25]; inhibition of antigen presenting cells activating conventional T cells via CTLA-4;[26, 27] as well as the production of immunosuppressive cytokines (IL-10, IL-35 and TGF-β)[28-30]. Various other immunosuppressive cells additionally exist in the tumour microenvironment – alongside Treg cells, B regulatory cells, cancer-associated fibroblasts, myeloid-derived suppressor cells, as well as vascular endothelial cells all additionally contribute to immunosuppression[, 31]. M2 macrophages, for example, have been found to be recruited to the colorectal carcinoma (CRC) microenvironment where they release immune-suppressive cytokines such as IL-10, thus further inhibiting any cytotoxic T cell response[32].

Tumour cells themselves can directly evolve mechanisms to escape immune-mediated killing, and this can take a myriad of forms. For example, through the downregulation of MHC class I, or by the upregulation of the expression of the T cell inhibiting ligand programmed death-ligand 1 (PD-L1) on the surface of tumour cells[33]. PD-L1 engages programmed cell death protein 1 (PD-1) on the surface of T cells, initiating phosphorylation-dependent inhibitory signalling within the T cell, countering activatory signalling via the TCR and co-stimulatory molecules, particularly CD28, thus inhibiting T cell-mediated anti-tumour activity[33,34]. Specifically, the intracellular tail of PD-1 contains the immunoreceptor tyrosine-based switch motif, which upon PD-1 engagement recruits the Src homology region 2-containing protein tyrosine phosphatase 2 (SHP2). SHP2 can dephosphorylate activated Zeta-chain-associated protein kinase 70 (ZAP70), phosphoinositide 3-kinase as well as Rat sarcoma virus (RAS), all mediators of positive TCR signalling. Resultantly, the activation of key transcription factors upon which T cell signalling converges upon, namely nuclear factor of activated T

cells (NFAT) and Nuclear factor kappa-light-chain-enhancer of activated B cells (NF-κB), is reduced and T cell effector functions are dampened[35-37].

It is the goal of cancer immunotherapy to combat such mechanisms, thus rendering a tumour cell susceptible to T cell-mediated killing[34]. Particularly important in the field of immunotherapy are the anti-PD-1 agents, namely pembrolizumab. Pembrolizumab is a monoclonal antibody targeting PD-1 on the cell surface of lymphocytes[34]. This biologic blocks PD-L1 on the surface of tumour cells from binding to PD-1, relieving the inhibitory signalling within the T cell, subsequently allowing T cell mediated killing of tumour cells[34]. In a phase II clinical trial of the anti-PD-1 immunotherapy pembrolizumab, the 20-week progression-free survival of patients with progressive metastatic MSI-H CRC was 78%[38]. This finding has since been replicated and pembrolizumab is licenced by the UK National Health Service (NHS). However, like most cancer treatments, checkpoint inhibition is effective only in certain clinical contexts and it is vital to stratify groups of patients based on their responsiveness to prevent the delivery of superfluous therapy[38]. For example, whilst the success of pembrolizumab is clear in MSI-H CRC, the same effect is not seen in micro satellite stable (MSS) patients who in the same study exhibited only an 11% progression-free survival[38]. It is vital to understand the mechanisms preventing patient response in order to develop methods rendering them susceptible to such therapies. In this particular case, an in-depth understanding of Microsatellite instability (MSI) is clearly necessary to bridge this gap in treatment response.

Mechanism of microsatellite instability

DNA replication is inherently susceptible to errors, with DNA polymerase generating an approximate error rate of approximately one mistake per 10^4 nucleotide pairs[39]. Whilst DNA

polymerase possesses intrinsic proofreading capabilities[40], cells rely heavily on their mismatch repair (MMR) system to rectify these errors. MMR orchestrates a complex interplay among multiple proteins tasked with the detection and correction of mismatched base pairs and insertion/deletion (INDEL) loops within DNA[41]. Specifically, MutS Homolog (MSH) 2 a key protein involved in the MMR pathway, engages in heterodimerization with either MSH6 or MSH3, depending upon whether the lesion arises from mismatched bases (in the former case) or INDEL loops (in the latter)[41]. This heterodimer harbours two ATPase active sites, which when bound to ATP and the mismatched base, induces a conformational change in the heterodimer, forming a sliding clamp capable of traversing along the DNA helix[42]. The ATP-activated heterodimer subsequently recruits another protein complex, MutLα comprised of MLH1 and Mismatch repair endonuclease PMS2 (PMS2), with the resulting machine known as the proliferating cell nuclear antigen[43]. Replication factor C loads this sliding clamp onto the DNA strand and activates MutLα to incise the mismatched region[44]. These enzymatic cleavages excise the error from the DNA, permitting DNA polymerase δ to commence the re-synthesis of the now-corrected DNA segment[9]. Subsequently, DNA ligase catalyses the ligation of the ends, thereby concluding the DNA repair process[45]. It is noteworthy that the MMR machinery additionally assumes an integral role in mediating DNA damage signalling[46]. This signalling function is manifested either through cell cycle arrest or programmed cell death[46], further ensuring genomic integrity, albeit the precise underlying mechanisms remain incompletely elucidated[46].

It is well established that defects in DNA repair proteins predispose to cancer[47]. For example, in colon cancer, germline mutations in the MSH2, 3, 6, MLH1 and PMS2 genes allow an accumulation of mutations which culminate in hereditary nonpolyposis colon cancer (HNPCC), also referred to as Lynch Syndrome, accounting for up to 5% of all colon cancer

cases[48, 49]. The majority of the sporadic cases are a consequence of BRAF V600E substitution which hypermethylates the MLH1 promoter, thereby reducing expression of the MLH1 and PMS2 proteins[50, 51]. Both mechanisms result in MMR deficiency (dMMR), which occurs with a frequency of approximately 15% in all colorectal cancer (CRC) patients[52].

Intuitively, inactivation of the system that repairs damages in DNA results in an accumulation of mutations, referred to as a mutator phenotype[53]. As a way of measuring this mutator phenotype, the stability of DNA microsatellites can be assessed[53]. A microsatellite is a region between 10-60 base pairs composed of a short repetitive DNA sequence ranging from between 1-6 base pairs and are found throughout the genome[54]. Microsatellite regions are prone to replication errors – when replicating these regions, DNA polymerase can slip over the repetitive sequences, changing the length of the microsatellite[54]. Despite this, the MMR machinery will usually correct such errors[16]. In the case, however, where a cell's MMR machinery is no longer proficient, these errors will not be corrected and will accumulate within the DNA, and whilst microsatellites are not coding segments of DNA and this has no functional effect on the cell, it provides a useful profile of MMR proficiency[54]. Consequently, dMMR results in a microsatellite instability high (MSI-H) phenotype. MSI-H has historically been defined as instability in at least two of the five Bethesda reference panel markers (BAT-25, BAT-26, D2S123, D5S346 and D17S250)[55]. Alternatively, if a tumour has only instability in one of the Bethesda markers, it is defined as MSI low (MSI-L)[55]. If there are no mutations within this panel, the tumour is categorised as MSI stable (MSI-S or MSS)[55]. Diagnostically, polymerase chain reaction (PCR) is the most common method used to analyse the length of the Bethesda markers in order to classify a tumour based on its MSI status[55].

As alluded to, the MSI status of a tumour has important consequences on the prognosis and outcome of different cancer treatments[56]. It is now well established that this is a consequence of MSI-H tumours having a greater immune infiltration than MSS tumours, owing to the high neoantigen burden of dMMR tumours which attracts tumour infiltrating lymphocytes[57]. Saeterdal and colleagues compared the immune infiltration of MSI tumours with MSS and found greatly enhanced $CD8^+$ T cell infiltration within the MSI-H subset[58]. To understand how an MSI-H tumour, initiates this immune infiltrated phenotype, Linnebacher and colleagues found that a frameshift mutation within the TGFβIIR gene in MSI-H CRC produces a frameshift peptide bound to HLA-A2[59]. The group found this frameshift peptide was capable of inducing a CD8+ T cell response as a consequence of its mutant sequence, which T cells do not recognise as 'self'[59]. Consequently, this study highlighted the ability of frameshift peptides to initiate an anti-tumour immune response[59].

Interestingly, within MSI-H tumours, there are a subset of patients who do not respond to immunotherapies. A recent phase III clinical trial of pembrolizumab vs chemotherapy found that within advanced MSI-H stage IV CRC, approximately 50% of patients failed to respond to checkpoint blockade[60]. This finding suggests an immune resistance against checkpoint blockade, which is vital to investigate to better understand predictive biomarkers of response, as well as for the development of improved immunotherapeutic approaches[60]. To uncover genetic mechanisms of immune evasion in CRC, Grasso et al. performed a multi-omic analysis of over 1000 primary colorectal tumour samples[61]. Within MSI-H tumours, a general enrichment for mutations in the antigen presentation machinery (APM) was observed[61]. 57% of all MSI-H tumours displayed at least one mutation in the HLA-A, -B, or -C genes, whilst 11% of the samples contained biallelic mutations in the β2-microglobulin (β2M) gene[61]. β2M is a small protein which stabilises MHC-I molecules, as well as assisting their folding and

assembly, therefore its mutation results in loss of cell surface MHC-I expression[62]. A third vital member of the APM is the Transporter Associated with Antigen Processing (TAP) family of proteins. TAP1 in complex with TAP2 forms an ATP-dependent peptide transporter which translocates cellular peptides to the endoplasmic reticulum where they are processed and loaded onto MHC-I molecules[63]. Moreover, TAP2 is vital in ensuring MHC-I molecules are correctly folded and bound to peptide before allowing their transport to the cells surface[63]. Intuitively, loss of TAP function significantly impairs antigen presentation, and within MSI-H CRCs, the TAP2 gene observed a biallelic mutation frequency of 8%[61].

It is vital to note the importance of natural killer (NK) cells in this context. NK cells are innate immune cells with a vital role in detecting cells that have lost MHC-I expression[64]. The primary NK cell inhibitory receptors belong to the killer cell immunoglobulin-like receptor (KIR) family[64]. These receptors bind MHC-I molecules, initiating inhibitory signalling within the NK cell therefore preventing its activation[64,65]. If this inhibitory signalling is alleviated as a consequence of missing MHC-I, the NK cell will activate inducing 'self'-recognition[64]. This activation eliminates target cells via either direct cytotoxicity or mediated via the proinflammatory cytokines Tumour Necrosis Factor alpha (TNF-α) and Interferon gamma (IFN-γ)[64]. Consequently, loss of MHC-I expression in the context of cancer should trigger NK cell activation[66]. Immune exclusion is one mechanism by which tumours surpass this issue, and in CRC the number of infiltrating NK cells has been shown to be significantly reduced compared to normal tissue[68].

Mechanisms of antigen presentation

As already alluded to, antigen presentation is an opportunity for a cell to report its ongoings to the immune system. When a cell is infected with a virus it will usually begin translating

viral proteins as part of the viral replication process[69]. Viral proteins can be tagged with ubiquitin as a consequence of inherent cellular folding errors and targeted for degradation within the cell and peptides derived from these proteins are presented on the cell surface via the classical human leukocyte antigen (HLA) pathway[69]. These peptides are bound to the HLA class I gene products, HLA-A, B and C. $CD8^+$ T cells of the immune system are selected during their development so that they recognise peptides that are non-'self', priming the T cell to attack and kill the virally infected cell, thus eliminating the virus[70]. Viral peptides tend to be stable with low turnover rates, yet $CD8^+$ T cells are able to recognize and kill a virally infected cell within one hour[69]. This finding suggested that antigen presentation was not dependent on the natural turnover of proteins[71] and the defective ribosomal product (DRiP) hypothesis was established. DRiPs are polypeptides that arise as a consequence of errors in either translation or post-translational processing[72]. They are unable to reach their mature conformation and therefore must be degraded to prevent the formation of potentially toxic aggregates. Since their initial definition, the DRiP designation has progressed, now including protein products generated owing to errors in transcription, splicing, and translation[73]. It has been estimated that DRiPs account for up to 30% of newly synthesized proteins[74]. Peptides can also be presented by the major histocompatibility complex (MHC) class II pathway – these are derived from extracellular proteins which are transported into the cell in a phagosome[75]. Intracellularly, the phagosome fuses with a lysosome which displays an acidic pH, allowing the breakdown of the protein contents[75]. This fuses with an endosome containing MHC class II which once bound to peptide traffics to the cell surface.[75]. MHC class II molecule gene products consist of HLA-DR, DP and DQ, which are restricted in their expression and are recognised by CD4+ T helper cells[75].

DRiPs are generated by a number of means, and their frequency is increased in the context of cancer, particularly in patients with MSI-H tumours[73]. dMMR, as discussed above, allows the accumulation of mutations within the genome, many of which disrupt the amino acid reading frame[53]. Such frameshifts can, for example, result in the loss of a stop codon, consequently producing a defective mRNA[73]. The absence of this stop codon results in ribosomal stalling during translation and produces a defective polypeptide product[73]. As this polypeptide originates from defective mRNA, its degradation is vital in order to prevent any aberrant functions that it may have consequently acquired from mutation. The removal of this defective polypeptide product is orchestrated by the ubiquitin-proteasome system (UPS)[76].

The ubiquitin-proteasome system

The UPS is the primary pathway for polypeptide degradation. It is a tightly regulated and evolutionarily conserved pathway, crucial in regulating the expression levels of a wide range of proteins[76]. Namely, the UPS centres around ubiquitin – a 76-amino acid long protein found in all eukaryotic cells[78, 79]. The many functions of ubiquitin require its conjugation to a target molecule, the orchestration of which requires a plethora of different mediators[76]. Briefly, the UPS can be categorised into three stages: ubiquitination, proteasomal degradation and ubiquitin recycling[76]. Firstly, ubiquitination relies on the joint action of three ubiquitinating enzymes: E1 ubiquitin-activating enzymes, E2 ubiquitin-conjugating enzymes, and E3 ubiquitin-ligating enzymes[76, 78, 79]. Firstly, the E1 enzyme uses the energy generated from the hydrolysis of ATP to activate the C-terminal carboxyl group of ubiquitin through acyl-adenylation[76]. Subsequently, E1 transfers the activated ubiquitin to an E2 enzyme which forms a thioester bond between the ubiquitin and the E2's catalytic cysteine residue[76]. This E2-ubiquitin conjugate then associates with an E3 enzyme, which creates an isopeptide bond between the C-terminal glycine of the activated ubiquitin and a lysine residue at the C-

terminus of the target protein[76]. The polymerisation of ubiquitin on a polypeptide culminates in a ubiquitin chain, the presence of which serves as a signal for the polypeptide to be shuttled to the proteasome[76].

The repertoire of E2 and E3 enzymes varies between organisms, with humans encoding 35 different E2 enzymes, and 377 different E3 enzymes[80]. Within the E3 family, diversity maps to the catalytic domain, which can be categorized into three major types: Ring-Between-Ring (RBR), Homologous to E6-AP Carboxyl Terminus (HECT), and the Really Interesting New Gene (RING) domain[80]. Each domain exhibits distinct mechanisms of ubiquitination, tuning protein regulation[80].

Upon the arrival of a ubiquitinated polypeptide at the proteasome, its proteolytic cleavage is initiated. The proteasome is a large, barrel-shaped molecular complex, composed of a catalytic core and either one or two terminal 19S regulatory particles[76]. The 19S regulatory particles contain a lid complex which is composed of several non-ATPase subunits, the primary function of which is to deubiquitinate ubiquitin tagged polypeptides[76]. This ensures ubiquitin recycling, which can then be used to ubiquitinate other polypeptides[76]. After recognition and deubiquitination, the substrate continues to the core of the proteasome which contains the proteolytic activity responsible for cleaving ubiquitin tagged polypeptides into oligopeptides[76]. These oligopeptides typically consist of amino acid chains approximately 3-15 residues in length and can be either further degraded, or processed for presentation on the cell surface via the MHC I pathway[76].

Ribosomal Quality Control

A particularly important process that provides with ubiquitinated substrates to the UPS is the ribosomal quality control (RQC). The RQC pathway is a vital cellular process that operates in eukaryotic cells to ensure the fidelity of protein synthesis and maintain protein homeostasis in a process related but distinct to co-translational ubiquitylation[71]. This pathway is responsible for identifying and resolving problems that can occur during translation caused by stalled ribosomes that encounter problematic sequences or structures in the mRNA template, rare codons or issues with tRNA availability[71]. Such sequences arise as a consequence of aberrations within mRNA[71]. For example, if a stop codon is lost through endonuclease cleavage or by premature polyadenylation, the mRNA becomes nonstop. This results in ribosomal stalling, and it's the role of the RQC pathway to disengage such stalled ribosomes, recycling their subunits for future use[71]. In doing so, the RQC pathway must extract the nascent polypeptide, directing it for proteasomal degradation[71].

Primarily, the RQC pathway operates within the cytosol, however it is of note that there are distinct RQC mechanisms operating in the endoplasmic reticulum (ER)[71]. For example, the ER-associated degradation pathway ensures that protein synthesis within the ER produces correctly folded, functional proteins[71]. Any nascent protein failing to reach its correct conformation within the ER must be retrotranslocated and targeted for proteasomal degradation[71]. Whilst a number of parallels can be drawn between ER and cytosolic RQC, it is important to distinguish these two separate mechanisms.

Cytosolic RQC is a conserved pathway in eukaryotes[81]. RQC mainly functions to monitor translation within a cell in a mechanism distinct from pathways which monitor polypeptide folding state[81]. This pathway is triggered when a ribosome becomes stalled during translation, which can be detected by one of two mechanisms. In the first instance, stalling can be

recognised by the ubiquitin ligase Zinc Finger Protein 598 (ZNF598), which identifies collided ribosomes[82]. ZNF598 is an E3 ubiquitin ligase and when recruited to the ribosomal 40S subunit, it ubiquitinates the 40S ribosomal proteins S10 and S20[71,82]. The ubiquitination of these proteins recruits the activating signal co-integrator complex, splitting the subunits of the stalled ribosome[82, 83]. Alternatively, stalling can be detected by recognition of an empty ribosomal A site – if a non-stop codon is encounter during translation, the ribosome will reach the 3' end of the mRNA template, and the A site will be left empty[83]. Resultantly, the protein Pelota is recruited, which along with its partner proteins ABEC1 and Hbs1, results in the separation of the two ribosomal subunits[84]. The 40S ribosomal subunit can then be recycled for further translation. Importantly, exoribonuclease 1 works with the exosome complex to degrade the defective mRNA, ensuring no further translation of this template can ensue[85].

After the stalled ribosome has split into its constituent subunits, the large 60S subunit remains bound to the nascent polypeptide chain conjugated to tRNA[82]. Resultantly, this aberrant stalled subunit is detected[86] initiating the RQC pathway, outlined in Figure 1. Ribosome quality control complex subunit 2 (Rqc2) is firstly able to detect the aberrant structure through its simultaneous binding to both the 60S ribosomal subunit and the exposed tRNA[86]. Rqc2 binding recruits listerin E3 ubiquitin protein ligase 1 (LTN1) allowing its binding to the 60S ribosomal subunit. LTN1 is an E3 ubiquitin ligase, that catalyses the addition of ubiquitin onto lysine residues towards the C-terminus of the nascent polypeptide[86]. Polypeptide ubiquitination recruits the tRNA endonuclease ankyrin repeat and zinc finger peptidyl tRNA hydrolase 1 which releases the tRNA-bound nascent polypeptide, allowing polypeptide extraction from the ribosome by the AAA+ ATPase valosin-containing protein (VCP)[87,88]. The defective nascent polypeptide, is ready for degradation by the proteasome.

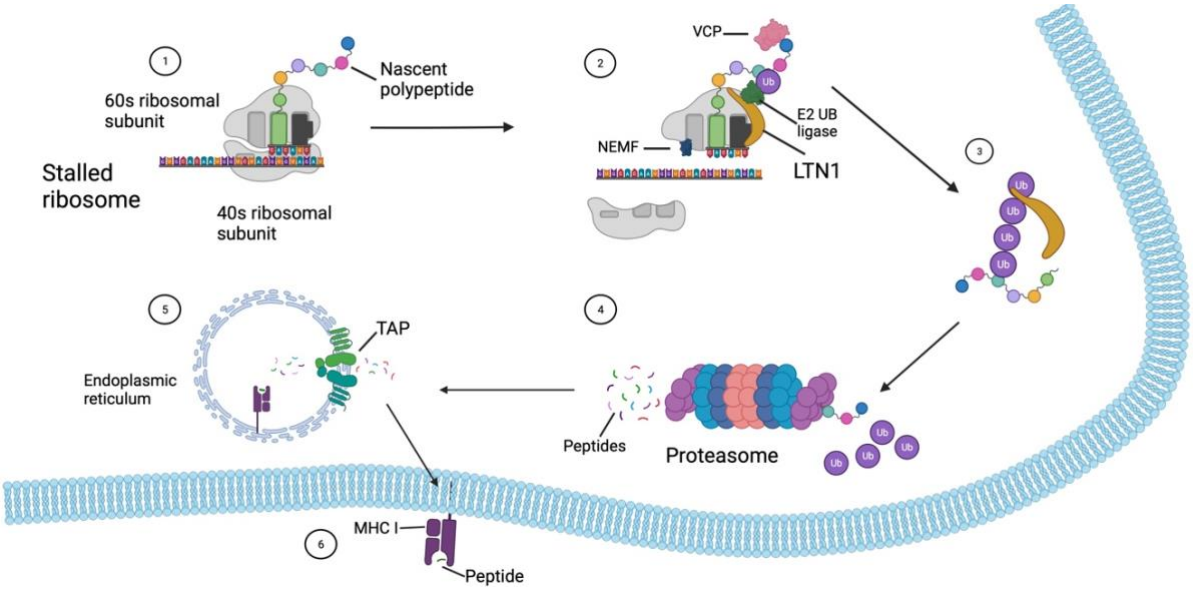


Figure 1.

Overview of the RQC pathway. RQC is initiated upon stalling of a ribosome by nonstop mRNA. This results in subunit dissociation, which recruits NEMF to bind to the 60S ribosomal subunit. NEMF recruits the LTN1 protein which in combination with an E2 ubiquitin ligase, ubiquitinates the nascent polypeptide. The ubiquitinated polypeptide is extracted from the ribosomal exit tunnel by VCP and sent to the proteasome for degradation into smaller peptides. The resulting peptides are transported via TAP into the ER where they are packaged onto MHC class I molecules and subsequently presented on the cell surface.

In cases where the nascent polypeptide has no lysine accessible to LTN1, the nuclease export mediator factor (NEMF) in collaboration with the large ribosomal subunit, can facilitate the addition of carboxy-terminal alanine and threonine residues, forming a C-terminal addition to translation (CAT) tail. This resultant CAT tail, propels the nascent polypeptide from the ribosome, providing a substrate for LTN1 ubiquitination[89, 90].

Not only does LTN1 have an important role in non-stop decay, but it has also been implicated in nonsense-mediated mRNA decay[71], whereby an mRNA transcript contains a premature

stop codon. Several mechanisms can activate nonsense-mediated decay, however the involvement of RQC in this process remains unclear[73]. A study investigating nonsense-mediated decay in yeast showed an involvement of LTN1-dependent RQC in the degradation of a truncated peptide, however this does not hold true for all nonsense mRNA and suggests degradation may be dependent on the specific mRNA[91, 92]. Consequently, it is clear that whilst much remains to be understood about the degradation of defective mRNA, LTN1 has a seemingly prevalent role.

The importance of LTN1

In a cornerstone study investigating LTN1, Trentini et al. found LTN1 to be an essential mediator of non-stop protein RQC[93] Through experimentally knocking out the LTN1 protein from HeLa cells, the group found loss of LTN1 significantly altered the immunopeptidome[93]. Specifically, a significant reduction (between 2- to 105-fold) was observed in the expression of 103 peptides, reflecting approximately 3% of the experimentally detected immunopeptidome[93]. Specifically, within the differentially presented peptides, the group identified a number of multipass transmembrane proteins, which appear to be an important target of LTN1[93]. From this, it is clear that LTN1 is an important regulator of antigen presentation. These results were established in HeLa cells, and whilst they provide useful insight into the peptides LTN1 may be responsible for degrading, the results are cell line specific[93]. In order to add clinical significance to this data, a more relevant cell line should be used, reflecting the differences in the peptidome of a specific cancer subtype.

In an effort to uncover novel therapeutic targets for colon cancer, Vasaikar et al. performed a proteogenomic study on over 100 human colon tumour samples[94] Interestingly, the group demonstrated that LTN1 was among the most common and highly mutated genes, with a

mutation frequency of 60% in the MSI cohort[94]. These mutations result primarily in translational frameshifts which introduce an early stop codon, thus truncating and inactivating the protein[94]. The mutant peptide produced as a consequence of a frameshift is degraded and can be presented on the cell surface[94]. Due to the frameshift, the peptides derived from this protein are different from those derived from the wildtype protein, therefore these peptides are neoantigens. Consequently, frameshift peptides derived from the inactivation of tumour suppressor genes are a major source of neoantigens.

A recent study from Ballhausen et al. describing the landscape of frameshift peptides in MSI-H tumours identified frameshift neoepitopes derived from LTN1 gene in MSI-H CRC[95] Intriguingly, the group proposed that the frameshift neoepitopes derived from LTN1 are immunogenic[95]. The group vaccinated HLA-A*02:01 transgenic mice with the identified LTN1-derived frameshift epitope, and IFNγ enzyme-linked immunosorbent spot (ELISpot) assays revealed an immune response within the mice[95]. The prediction that LTN1-derived peptides may be presented in a high percentage of MSI-H CRC patients asks whether LTN1-derived frameshift peptides could be potential targets of immunotherapy efforts.

Importantly, this study demonstrated that dMMR cancers share a pool of frameshift peptides (FSPs). The identification of such frameshift neoantigens is a vital area of current research, informing the development of cancer therapies, such as neoantigen-based vaccines against MSI cancers[59]. As frameshift mutations are often shared between cancers of the same subtype, these recurrent FSPs are candidates for preventative cancer vaccines.[59] Within MSI CRC, FSPs have been found to be immunogenic, resulting in CD8+ T cell activation[59, 96]. This finding has culminated in the development of FSP vaccines directed against MSI CRCs – a number of which have proven safe in early clinical trials[101] Despite this, any preventative

effect has yet to be observed. Through combining rigorous in silico prediction methods with in vivo immunogenicity testing, Gebert et al. generated a FSP-derived vaccine based on four FSPs which when delivered to a mouse model of dMMR CRC resulted in an enhanced adaptive immune response and a resulting reduced tumour burden[98] Such preventative vaccines are especially vital in this tumour context as a consequence of the immune evasion mechanisms employed during later tumour development. Implicating LTN1 in this pool of neoantigens suggests that frameshift peptides derived from LTN1 itself could be a potential target for the development of a cancer vaccine. Despite this, there is currently no evidence that peptides derived from LTN1 are presented in human MSI-H CRC.

The structure of LTN1

LTN1 is a large protein with a generally conserved structure[99], however there are different variations of the gene sequence. The two main isoforms of the protein have either 1766 or 1,812 amino acids[100], with the former being the sequence used experimentally in the present study. A third isoform of LTN1 has been described (missing 439-1766 aa), lacking the catalytic E3 ligase activity[100]. LTN1 contains 16 HEAT repeats and one catalytic Zinc finger domain, found at the C terminus of the protein[100]. The Zinc-finger domain is a RING domain, which underlies E3 activity through acting as a binding site for E2 enzymes[101] In a structure-based study into LTN1 activity, Doamekpor et al. (2016) found that whilst the N-terminal domain has no impact on the ability of LTN1 to ubiquitinate a protein, LTN1 binds to the 60S ribosome through its N-terminal domain, and the protein cannot perform its function in vivo without an intact N-terminal domain[102]. LTN1 protein has an elongated structure which allows the N-terminal domain to only bind the 60S ribosomal subunit when the 40S subunit is not present, preventing aberrant RQC activation, whilst positioning the RING domain so it can ubiquitylate the nascent polypeptide[102].

RQC generates neoantigens

RQC ensures that nascent polypeptides originating from mutant mRNA are degraded and subsequently presented on the cell surface[73]. The mutant mRNA can harbour INDELs which result in a frameshift of the amino acid reading frame; thus, the sequence of the resultant polypeptide is different from wildtype[73]. The degradation of these polypeptides thus generates neoantigens which are bound to MHC class I and are presented on the cell surface as a fingerprint of the cell.

Hypothesis

Unpublished analysis of whole genome sequencing data from approximately 1000 CRCs from Genomics England (Dr. D Church, Nuffield Department of Medicine, University of Oxford) has identified LTN1 to contain a silencing mutation at a frequency of approximately 20%, mostly within MSI-H tumours. Frameshift mutations in LTN1 within CRC have additionally been identified at a higher frequency by other groups[103]. Frameshift mutations generate frameshift peptides which are immunogenic when presented – these are frequently derived from the RQC pathway.[59, 96] Consequently, tumours containing mutations within genes involved in the RQC pathway, for example LTN1, will prevent the presentation of RQC-derived immunogenic neoantigens, thus escaping immune editing.

We hypothesize that frameshift mutations in the LTN1 gene within the MSI-H group of tumours occur as an immune evasion mechanism during tumour progression. Abrogating LTN1 E3 ligase activity prevents the RQC-mediated degradation of mutant nascent polypeptides, disrupting HLA class I-mediated antigen processing. Consequently, neoantigen presentation is prevented, interfering with T cell-mediated elimination of MSI-H cell clones

carrying immunogenic frameshift peptides (neoepitopes). We hypothesize that these mutations occur within the MSI-H group of CRC patients that do not respond well to cancer immunotherapies, as a consequence of LTN1 mutation successfully hiding the tumour from the immune system, rendering immunotherapies ineffective.

Studying the immunopeptidome of tumour cell lines and primary tumour samples containing mutations within LTN1 is an important approach for specifically understanding the role of LTN1 in tumour antigen presentation. As frequent mutations in LTN1 have been described in CRC, it is vital to directly examine the role of LTN1 within the context of a CRC model to implicate the specific cancer associated antigens LTN1 is responsible for the degradation and presentation of, ensuring the clinical translatability of this data. To this end, the mutational status and expression profile of LTN1 in MSS and MSI-H CRC cell lines was first determined. From this, an appropriate model for the investigation of LTN1 function was selected. To understand the impact of LTN1 on the global immunopeptidome, LTN1 was transfected into the established cell line model and the effect on MHC-I expression was quantified. This project provides the foundation for the optimisation of a stable cell line expressing the LTN1 protein and will enable future immunopeptidome profiling to determine the contribution of LTN1 to the CRC immunopeptidome.

MATERIALS AND METHODS

Cell Culture

All cell culture work was performed in a Class II laminar flow hood using standard aseptic techniques and cells were maintained at 37°C and 5% CO_2 in a humidified cell culture incubator. All cell lines were maintained in their respective media (Table 1), and passaged when reached 70-90% confluency. Cells were quantified with an automated cell counter

(Biorad), using Trypan blue (Thermo Fisher Scientific) for dead cell exclusion. Adherent cells were detached by incubation with TrypLE Express Enzyme (Gibco) at 37°C for approximately 3 minutes. All cell lines used in this study were subjected to mycoplasma testing and their authenticity was verified by Short Tandem Repeat (STR) analysis (Eurofins). Cell lines were sourced either from online suppliers or obtained from collaborating laboratories.

Table 1. Human Colorectal cell lines used in the study and their growth media

Cell line	**MSS/MSI Status***	**Growth medium**
COLO-320	MSS	RPMI-1640 Medium + 10% FBS
HCT-116	MSI	McCoy's 5a Medium Modified + 10% FBS
HT-29	MSS	McCoy's 5a Medium Modified + 10% FBS
HT-115	MSS	Dulbecco's Modified Eagle Medium + 15% FBS
LOVO	MSI	Eagle's Minimum Essential Medium + 10% FBS
LS-180	MSI	Eagle's Minimum Essential Medium + 10% FBS
SNU-104-	MSI	RPMI-1640 Medium + 10% FBS
SW278	Unknown	Dulbecco's Modified Eagle Medium + 20% FBS
SW40	Unknown	Dulbecco's Modified Eagle Medium + 20% FBS
SW48	MSI	Leibovitz's L-15 Medium + 10% FBS

* Microsatellite stability information obtained from https://cellmodelpassports.sanger.ac.uk and https://web.expasy.org/cellosaurus

Flow cytometry

All adherent cells were detached from culture flasks using Non-Enzymatic Cell Dissociation Solution (Merck) to preserve integrity of membrane surface proteins. A total of $1x10^6$ cells were used per staining reaction. Antibodies were used at previously established optimal

dilutions, with staining performed on ice for 30 minutes. The antibodies used were directed against HLA class I, HLA-A2. A viability stain was included in all reactions. Samples were fixed with 2% paraformaldehyde for 15 minutes at room temperature, and ran immediately after fixation on either a Attune (Thermo Fisher Scientific) or a BD LSRFortessa (Beckton Dickinson).

For intracellular staining, again a total of $1x10^6$ cells per reaction were used. Cells were resuspended in BD fixation/permeabilization solution and incubated at 4°C for 20 minutes. Subsequently, the permeabilized cells were washed with BD Perm/Wash buffer and incubated with an unconjugated anti-LTN1 antibody for 30 minutes at 4°C. Following this, cells were washed and incubated with an appropriate fluorochrome conjugated secondary antibody, for 30 minutes at 4°C.

Results were analysed with FlowJo v10.10.0

Table 2. List of Antibodies used for flow cytometric analysis.

Antibody	Clone	Host/Isotype	Conjugate	Source
HLA-A,B,C	W6/32	mouse IgG2a	Pacific Blue	Biolegend
HLA-A2	BB7.2	mouse IgG2b	APC	Biolegend
LTN1	polyclonal	rabbit/IgG	unconjugated	Atlas Antibodies
anti-rabbit	polyclonal	goat/IgG	APC	Life Technologies
Fixed Viability Kit			Zombie Nir	Biolegend

Protein Preparations and Western blot Analysis

Prior to the western blot analysis cells were lysed in lysis RIPA buffer (1% NP-40, 0.1% SDS, 0.5% Na Deoxycholate, 1X PBS, made in H_2O), supplemented with Protease Inhibitors' cocktail for 20 minutes on ice with mild shaking. Precipitates were removed by centrifugation

at 12,000 revolutions per minute (rpm) for 20 minutes at 4°C. The Pierce BCA Protein assay kit (Thermo Fisher Scientific) was used to calculate protein concentration in cell lysates. A standard curve of protein concentration using bovine serum albumin (BSA) as standard was created by measuring protein absorbance at 595 nm in the CLARIOstar plate reader (BMG Labtech). From this, the volume of each sample corresponding to 40 µg of protein was calculated. This was topped up to a total volume of 10 µL using RIPA buffer, and 10 µL of 2X NuPAGE reducing buffer was added. Samples were mixed and denatured at 95°C for 5 minutes, followed by centrifugation at 16,000 g for 5 minutes at 4°C. 20 µL of each sample was loaded into a 2-8% acrylamide gel and a constant voltage of 150 V was applied across the apparatus for 45 minutes, submerged in loading buffer. The gel was then sandwiched with an activated membrane in the transfer apparatus, over which 20 V was applied for one hour. The membrane was then blocked in 5% milk for one hour to block non-specific binding, and then incubated in primary antibody on a rocker at 4°C overnight. The membrane was then washed in PBS-T every 10 minutes for 30 minutes, and then incubated in secondary antibody (Goat, anti-Rabbit, LI-COR) for 90 minutes. After washing with PBS-T (0.1% Tween), the membrane was visualised using the ChemiDoc MP Imaging System. After visualisation, the membrane was washed in blocking buffer on a rocker for one hour, after which a loading control antibody, GAPDH (Invitrogen), was added and the membrane was incubated on a rocker for one hour. The membrane was then visualised using ChemiDoc MP Imaging System.

Table 3. List of Antibodies used for Western Blot Analysis

Antibody	Clone	Host/Isotype	Conjugate	Source
LTN1	Polyclonal	rabbit/IgG	Unconjugated	ThermoFisher
GAPDH	GA1R	Mouse/IgG1	DyLight 680	ThermoFisher
anti-Rabbit	Polyclonal	goat/IgG	IRDye 800CW	LI-COR

Transient Transfection for Protein Expression

For transient plasmid transfection to generate either lysates for Western Blot or Flow Cytometry analyses, HCT116 cells were seeded in 6-well plates (Corning) and allowed to grow overnight to reach 40-60% confluency by the time of transfection (usually within 18-20 hours post seeding). When cells reached the desired confluency, they were washed once with sterile PBS before the addition of low serum media (5% FBS and no antibiotics). Cells were then transfected with plasmid(s) of interest using the transfection reagent Fugene HD (Promega) as per manufacture's recommendations. In brief, in a 1.5 mL tube, 2 µg of plasmid was diluted in 100 µL with Opti-MEM serum-free medium (Gibco) and mixed by gentle flicking. 6 µL of Fugene was then added and gently mixed by flicking, followed by 15-20 minutes incubation at room temperature. The plasmid solution was then added drop-wise to the wells and incubated at 37 °C and 5% CO_2 in a humidified cell culture incubator. 48 hours post-transfection, cells were washed with PBS and harvested for downstream analysis.

Polymerase Chain Reaction (PCR)

All PCRs were performed using Q5 High-Fidelity DNA Polymerase (New England Biolabs) to obtain 50 µL of product. The template DNA sample volume was calculated to ensure a final concentration of 20 ng. Both the forward and reverse primers were designed by another researcher in the lab in order to hybridise and amplify the LTN1 gene, and annealing temperatures were estimated to be 65°C using the NEB ™ calculator. The template DNA was added to a reagent mixture containing 5X Q5 Reaction Buffer, 10mM dNTPs, 10uM forward primer, 10uM reverse primer, Q5 High-Fidelity DNA Polymerase and nuclease-free water, taking care to add the DNA polymerase last to minimise non-specific amplification. The reaction then underwent thermocycling using the conditions detailed in Table 4.

Table 4. Thermocycling conditions used for PCR.

Step	Temperature	Time
Initial Denaturation	98°C	30 seconds
	98°C	10 seconds
30 Cycles	65°C	20 seconds
	72°C	20 seconds
Final Extension	72°C	20 seconds
Hold	8°C	

Primer sequences:

- LTN1-p.N.536fs-Fwd: AACCTTAGATGTTGCTCTGACTTT
- LTN1-p.N.536fs-Rev: TGAAAAAACAGCTCACAACTTGGAG

This primer pair targets exon 10 of the LTN1 coding sequence. The resulting PCR product was cleaned and sent for Sanger sequencing to validate mutational status.

Agarose Gel Electrophoresis

Electrophoresis was used to separate PCR products. Agarose gels were prepared by dissolving UltraPure Agarose powder (Invitrogen) in 1X Tris acetate EDTA (TAE) buffer (Sigma) and 5 μL of SYBRSAFE DNA gel stain (ThermoFisher Scientific). 5 μL of each amplified PCR product was mixed 6:1with 6X gel loading dye (ThermoFisher Scientific) and loaded into wells of the gel and run at 100V The 1Kb Plus DNA ladder (New England Biolabs) was used as a marker to determine size of PCR products. UV transillumination was used to visualise the PCR products.

Sanger Sequencing

The Monarch PCR and DNA Clean-up Kit (New England Biolabs) was used to purify the PCR amplified products, as per manufacturer's instructions. Sanger sequencing was performed by a collaborating lab. The results were analysed using SnapGene software (Domatics).

Nucleic Acid Quantification

Nucleic acids were quantified using the Nanodrop (ThermoFisher Scientific). In brief, the correct detection was selected (either dsDNA or RNA) and the machine was blanked with 1 µL of the sample elution buffer. The pedestal was then cleaned and 1 µL of sample was added for quantification, recording the concentration as well as the A260/280, and A260/230 ratios.

RNA, cDNA synthesis and qRT-PCR

Real time quantitative PCR (RT-qPCR) was performed to provide insight into LTN1 mRNA expression in human colorectal cell lines. RNA extraction was performed using the Monarch Total RNA Miniprep Kit (New England Biolabs) as per manufacturer's instructions. RNA samples were used immediately or stored in -80°C until subsequent use.

For conversion of RNA to cDNA the UltraScript 2.0 cDNA Synthesis Kit (PCR Biosystems) was used following the manufacturer's recommendations. In brief, up to 50 ng of RNA was added to 10 µL of the master mix described in Table 5 using the thermocycling conditions described in Table 6.

Table 5. Master mix for cDNA Synthesis reactions

Reagent	Volume (µL)
5x cDNA Synthesis Buffer	2
20x Reverse Transcriptase	0.5

50 ng/µL RNA	1
H_2O	6.5

Table 6. Incubation conditions for cDNA reverse transcription kit.

Temperature (°C)	Time (minutes)
42	30
85	10

For the qRT-PCR reactions, a master mix was prepared using 2 ul of cDNA template, 10 µM of each relevant primer (described below) and qPCRBIO SyGreen Mix Lo-ROX (PCR Biosystems) and loaded to a MircoAmp Fast Optical 96-well plate (Applied Biosystems). The plate was loaded in to a QuantStudio 1 Real-Time PCR System (Thermo Fischer) and thermocycled as described in Table 7. Gene expression levels were normalised against GAPDH expression and fold change was calculated using the $2^{-\Delta CT}$ equation or $2^{-\Delta\Delta CT}$ [104].

Table 7. qRT-PCR Thermocycling Conditions.

Cycle	Temperature (°C)	Time (s)
1	95	120
40	95	5
	65	30

Primer sequences:

- LTN1-Fwd: TCAGGCTTATGCCAGAAAAT
- LTN1-Rev: ATGTGGTATGGAAGCATTGT

This primer pair targets exons 25-27 of the LTN1 CDS.

Plasmid Constructs

pCSDest and pCSDest with the LTN1 coding sequence was purchased from Addgene[105, 106] (Table 8). Lentiviral vectors expressing LTN1 and a coding sequence stuffer were purchased from Vector Builder. The coding sequence of LTN1 in the lentivector contained two silent point mutations (codon 1633 changed from CGA to CGC and codon 1762 changed from CGT to CGA) to introduce NruI restriction sites flanking the RING domain. Digestion with NruI and religation of the linear DNA to allow creation of a lentiviral plasmid encoding LTN1 with the RING domain deleted.

Table 8. Plasmids used in the study.

Name	Gene/Insert	Size (bp)	Bacterial selection marker	Depositing lab	Company	Vector ID
pCSDest	empty backbone	5808	Chloramphenicol and Ampicillin	Nathan Lawson	Addgene	22423
pCSDest_LTN1	LTN1	10,109	Ampicillin	Roger Reeves	Addgene	53855
pLV[Exp]-Bsd EFS>hLTN1	LTN1	12,722	Blasticidin	NA	Vector Builder	VB221129 -1228mwn
pLV[Exp]-Bsd-EFS>ORF_Stuffer	empty backbone	7670	Blasticidin	NA	Vector Builder	VB900123 -7817tsp

Bacterial Transformation

For propagation of plasmids, 10 ng DNA was added to a 16 µL aliquot of either NEB-5α bacteria, mixed and incubated on ice for 30 minutes. The cells were heat-shocked at 42°C for

30 seconds followed by a 2-minute incubation on ice. Subsequently, bacteria were cultured in 250 µL of S.O.C medium for 1 hour with shaking at 225 rpm. 30 µL of bacteria were innoculated onto ampicillin plates and incubated inverted at 37°C overnight. Individual colonies from overnight plates selected cultured overnight at 37°C and 225 rpm shaking.

Mini-prep Plasmid Extraction

To extract plasmid DNA, the QIAprep Spin Miniprep Kit (Qiagen) was used according to the manufacturer's protocol. In brief, bacterial cultures were pelleted by centrifugation at 5000 x g for 3 minutes. The supernatant was discarded and the pelleted bacteria were resuspended in 250 µL of Buffer P1 (with RNase A added). The cells were then mixed with 250 µL of Buffer P2, allowing lysis for 3 minutes. The lysis reaction was terminated by adding 350 µL of Buffer N3 and gentle mixing by inverting 6 times. Any precipitate in the mixture was pelleted by centrifugation at maximum speed for 5 minutes and the resulting supernatant was transferred into a QIAprep 2.0 Spin Column. After a 1 minute centrifugation, flow-through was discarded and the column was washed with 500 µL of Buffer PB, followed by another washing step with 750 µL of Buffer PE. The flow through was discarded and the column centrifuged at maximum speed for one further minute to remove any residual wash buffer. The column was transferred to a 1.5 mL collection tube and plasmid DNA was eluted in 50 µL of Buffer EB after one minute incubation at room temperature and a final centrifugation step for 1 minute.

Generation of the LTN1^{WT} and LTN1$^{\Delta RING}$ HCT116 stable expressing cell lines

HEK293 T cells were transfected with lentiviral plasmid DNA and second-generation lentiviral packaging plasmids, which included the psPAX2 containing gag and pol packaging vectors, and VSV-G, using Fugene transfection reagent. 48 hours post transfection, the

HEK293 T cell lentiviral supernatant was harvested and an optional concentrating step was included, consisting of centrifugation and continuous rocking overnight at 4°C. The resulting lentiviral supernatant was delivered to HCT116 using either traditional transfection or spin infection. 48 hours post transduction, HCT116 were allowed to recover for 24 hours, after which the process of Blasticidin selection was initiated.

Determining Blasticidin sensitivity of lentiviral transduced HCT116 cells

To determine the optimal concentration of Blasticidin concentration needed for selecting HCT116 cells positive for LTN1 expression, cells were incubated with a range of Blasticidin concentrations from 0-15 ng/μL and were harvested at various time intervals (0-14 days). Cell viability was assessed by flow cytometry using the Zombie Nir live/dead stain (Biolegend), and a standard curve of viability was generated.

Results

The HCT116 MSI cells are a naturally occurring knockout of the LTN1 protein

As alluded to, unpublished whole genome sequencing data from over 1000 human CRCs has identified the LTN1 gene to be mutated at a frequency of approximately 20% in MSI-H patients. The detected mutation is a recurrent frameshift deletion at the 536 amino acid position. This disruption to the amino acid reading frame introduces a premature termination codon. To study the biological significance of the observed LTN1 mutation in the CRC MSI patient cohort we aim to model the impact of LTN1 loss. To this end, selection of a biologically relevant cell line model system is vital to ensure the model translates to human clinical data. We first looked in published proteomic data from human tumour cell lines[61] to identify LTN1 protein expression profiles in MSS and MSI-H CRC cell lines. As shown in

Figure 2, LTN1 expression is greatly reduced in HCT116 compared to all other cell lines. Comparatively high LTN1 expression is seen in COLO-205, SW-403 and SW-948 cell lines.

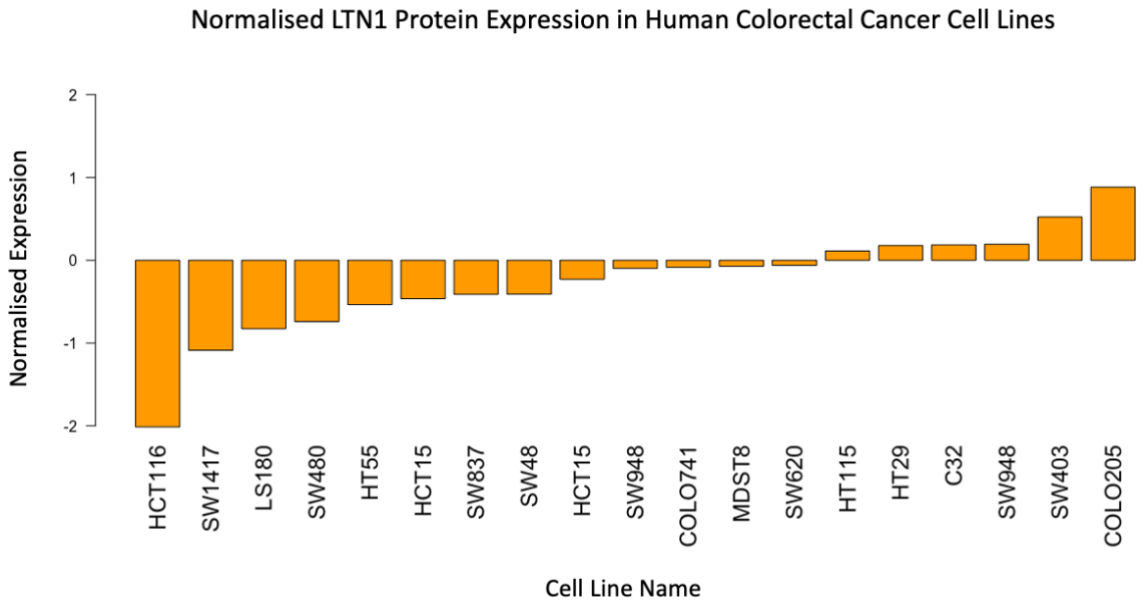


Figure 2

LTN1 expression is the lowest in the HCT116 cell line. LTN1 protein expression level in a selection of human CRC lines was analysed from publicly available quantitative multiplexed proteomics data[107]. Protein expression level was normalised by pooling the protein lysates of NCIH446, DMS79, NCIH460, DMS53, NCIH69, HCC1954, CAMA1, KYSE180, NMCG1, UACC257, and AU565 cell lines to represent the diversity in protein expression. LTN1 expression is the lowest in the HCT116 cell line and highest in COLO205 cells.

Due to prolonged cultivation in the laboratory, cancer cell lines can show genetic and phenotypic variations. Consequently, nine human CRC cell lines available for this study were profiled for LTN1 protein expression by western blot (Figure 3). Both MSS cell lines HT-29 and HT115 showed high LTN1 protein expression, as well as the MSI-H and MSI status unknown SNU-1040, SW48, LS-180, SW40 and SW278. Interestingly, two of the MSI lines, HCT116 and LOVO, showed no LTN1 protein expression.

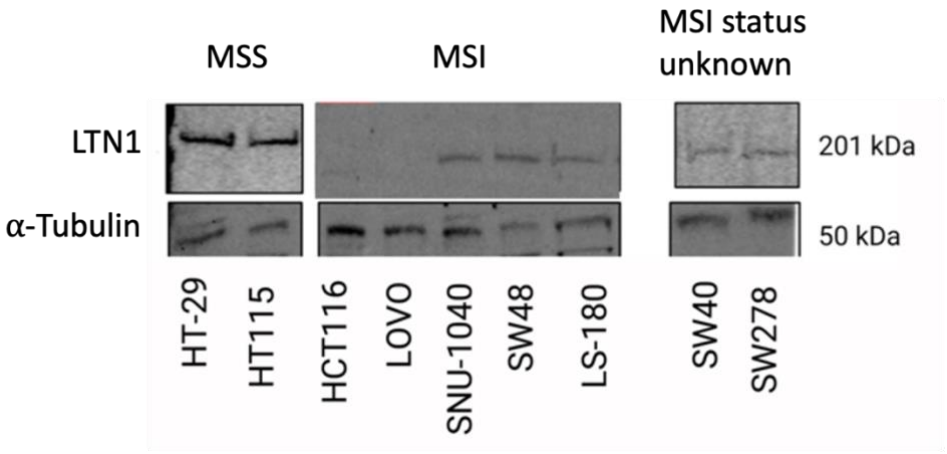


Figure 3

Western blot analysis confirmed undetectable LTN1 protein expression in HCT116. Cell lysates were extracted from available CRC cell lines and were subject to western blot analysis against LTN1 and the housekeeping protein α-tubulin. LTN1 expression in our cell lines matched the results shown in Figure 2 – LTN1 was undetectable in HCT116, expressed at a low level in LS180 and SW48, and highly expressed in HT-29 and HT115. SNU-1040 additionally exhibited low LTN1 expression. Cell lines were classified as either MSS, MSI, or their MSI status unknown based on microsatellite stability information obtained from *https://cellmodelpassports.sanger.ac.uk and https://web.expasy.org/cellosaurus*. Data collected in collaboration with Rose Faure.

LTN1 contains one microsatellite region which contains a series of 11 adenine nucleotides. Frameshift mutations within this microsatellite can arise as a consequence of dMMR where either one or two adenine molecules are deleted. This frameshift results in a premature stop codon which truncates the LTN1 protein which consequentially loses its catalytic activity. To confirm the mutational status of LTN1 in our CRC cell lines, this region was Sanger sequenced (Figure 4). Interestingly, HCT116 contains frameshift mutations in this microsatellite region in both copies of the LTN1 gene (p.N536M,fs*34, p.N536W,fs*2), referred to as a compound heterozygous genotype (Figure 4D). Combining this result with the

western blot data, it was hypothesized that the compound heterozygous mutation within the LTN1 gene in HCT116 resulted in a frameshift, disrupting the amino acid sequence of the LTN1 mRNA, truncating the protein and resulting in its loss of catalytic activity and subsequent degradation. Interestingly, the DNA strand containing the p.N536M,fs*34 mutation contains further downstream nucleotide changes at amino acid positions 537 and 539 which restore the wildtype amino acid. As these cell lines are MSI-H, they exhibit a mutator phenotype and the mutation of DNA downstream of the frameshift is likely a consequence of multiple independent mutational events occurring over time.

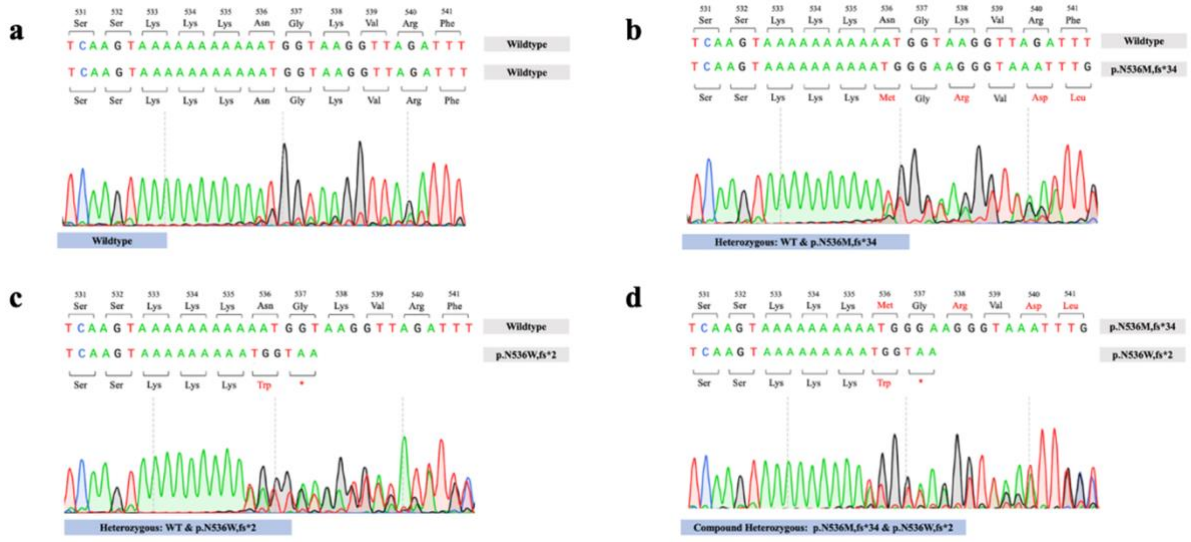


Figure 4

A compound heterozygous mutation was found within the DNA sequence of the LTN1 microsatellite region. (a) Wildtype LTN1 base pair sequence. (b) p.N536Mfs*34 heterozygous frameshift mutation and nucleotide change. (c) p.N536Wfs*2 heterozygous frameshift mutation. (d) Compound heterozygous mutation in LTN1 microsatellite with one allele harbouring the p.N536Wfs*2 mutation and one with p.N536Mfs*34, seen in HCT116. Data collected in collaboration with Rose Faure.

The present study aimed to investigate the role of LTN1 in MSI CRC tumours through assessing its contribution to the immunopeptidome. However, a common immune evasion mechanism within MSI tumours is the downregulation of HLA class I expression[108], therefore it was essential to determine whether the candidate tumour cell lines expressed sufficient MHC-I. To this end, flow cytometric analysis of panMHC class-I was performed on all CRC cell lines (Figure 5). Among the MSS cell lines, HT-29 expressed MHC-I, while HT115 did not. In the MSI-H cell lines, HCT116 and LS-180 exhibited MHC-I expression, whereas LOVO and SW48 did not. Analysis of the microsatellite instability unknown cell lines, both SW40 and SW278 expressed MHC-I. Combining this flow cytometry data, with the western blot and Sanger sequencing, HCT116 emerged as the most suitable cell line for investigating LTN1 function. HCT116 cells harbour a biologically relevant mutation in the LTN1 gene that is commonly observed in human MSI CRCs, therefore the transfection of LTN1 into HCT116 would rescue the recurrent mutation seen in human CRC. Consequently, this provides a biologically relevant model for the study of LTN1's function and the consequences of its loss.

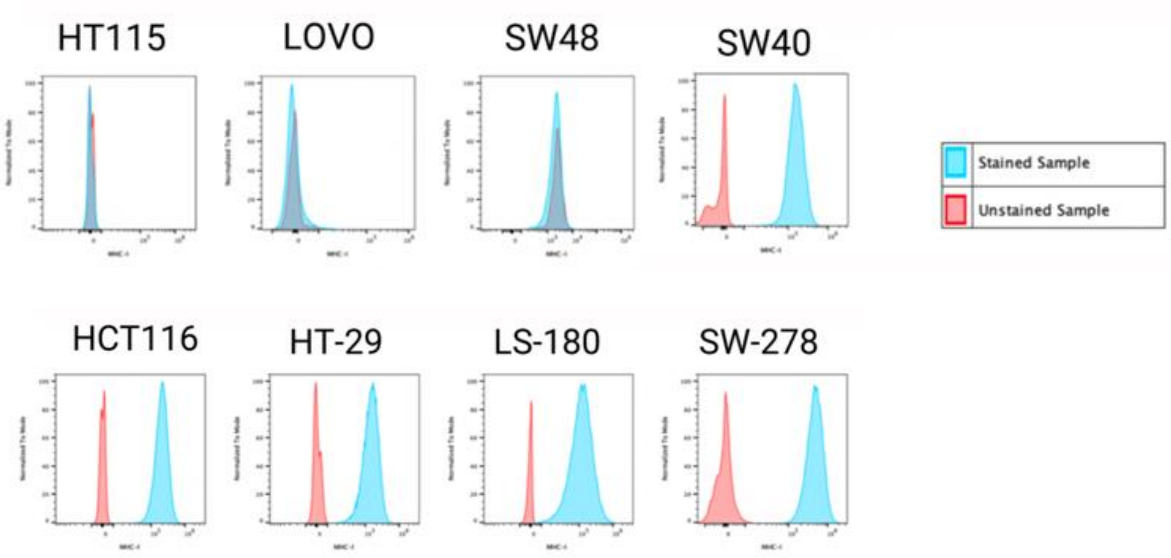


Figure 5

HCT116 cells abundantly express MHC-I. Cell surface expression of MHC class-I on CRC cell lines was assessed by flow cytometry. MHC-I was not expressed in HT115, LOVO and SW48. All other cell lines demonstrated MHC-I expression. Data collected in collaboration with Rose Faure.

MRNA expression levels of LTN1 in HCT116 cells

To understand the degradation mechanism of the LTN1 protein, RT-qPCR was performed to assess LTN1 mRNA levels in the different CRC lines (Figure 6). In accordance with the western blot data, HCT116 and LOVO cells exhibited low levels of LTN1 mRNA in comparison to HT29. Unexpectedly, SNU-1040 and SW40, despite expressing the LTN1 protein, expressed low levels of LTN1 mRNA, with the remaining cell lines being categorised as high LTN1 mRNA expressors. It is interesting that all cell lines tested express even small amounts of LTN1 mRNA, suggesting that these cells may be producing LTN1 protein which is rapidly degraded.

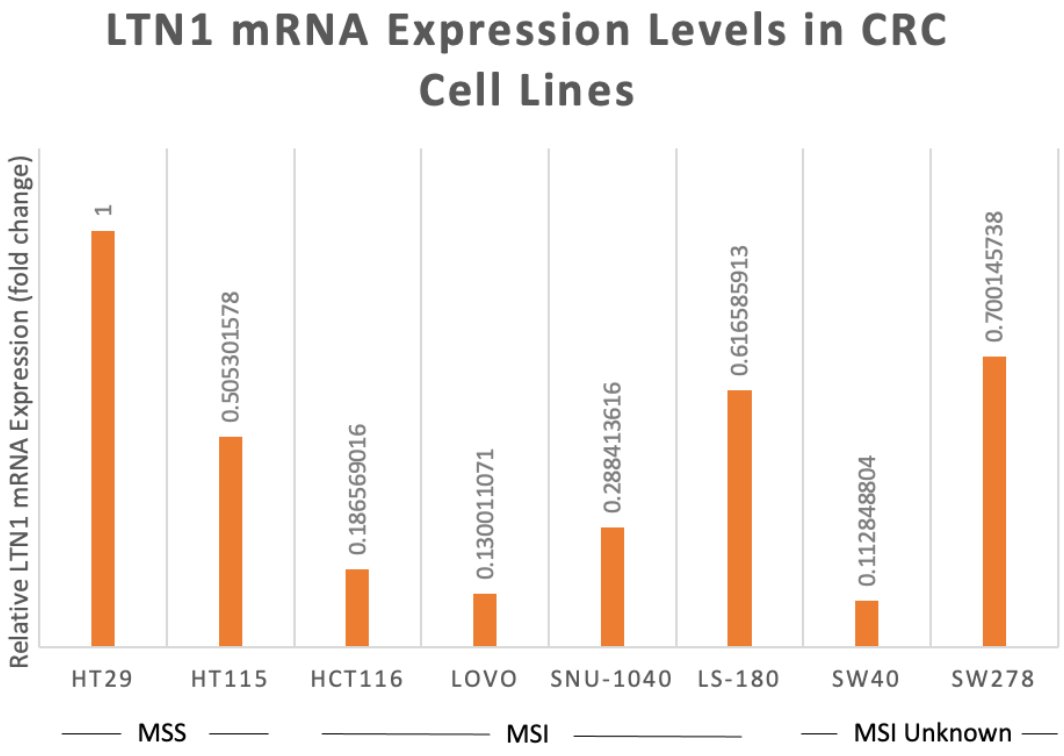


Figure 6

HCT116 express a small amount of LTN1 mRNA. mRNA expression levels of LTN1 were assessed in CRC lines by RT-qPCR analysis. HT-29 express the highest amount of LTN1 mRNA, with HT115m LS-180 and SW278 expressing a relatively high amount. LTN1 mRNA was greatly reduced in HCT116 cells, LOVO, SNU-1040 and SW40. Relative gene expression was calculated using the 2-ΔΔCt method, using GAPDH mRNA expression as reference gene and the MSS cell line HT29 as the calibrator.

Transient LTN1 expression in HCT116 upregulates MHC-I expression

Based on the observation from Trentini et al., that LTN1 knockout reduces the presentation of over 100 distinct peptides in HeLa cells[46], we sought to investigate the impact of LTN1 loss on MHC-I expression in HCT116 cells. Consequently, LTN1 was transiently transfected into HCT116, and panMHC-I as well as HLA-A2 expression were determined via flow cytometry. To control for any effects of the transfection procedure, HCT116 were separately transiently transfected with an empty vector (EV). Transfection of LTN1 into HCT116 cells resulted in upregulation in both panMHC-I and in the HLA-A2 allele as compared to the WT HCT116 and HCT116 transfected with the control EV (Figure 7).

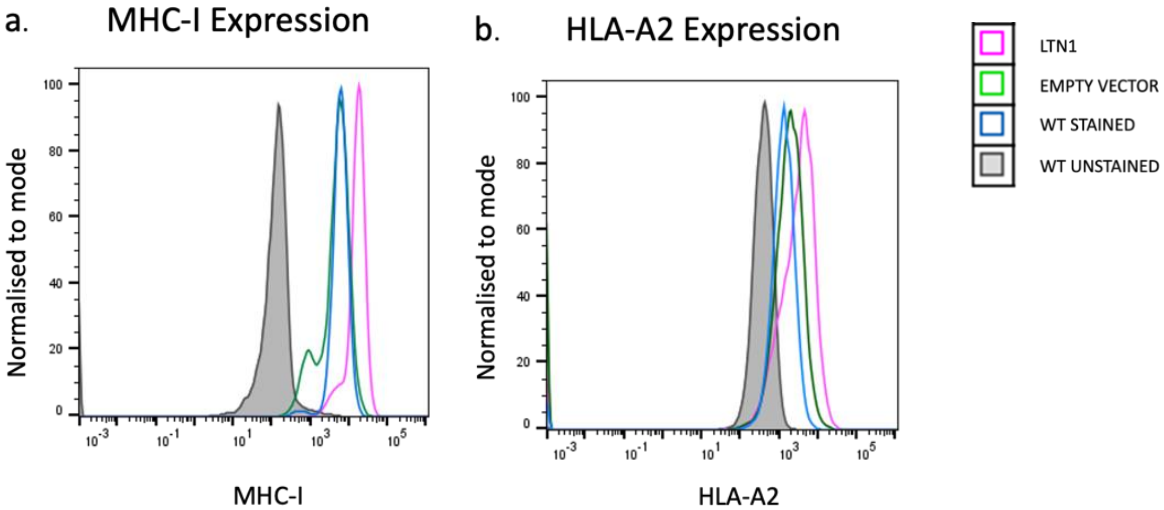


Figure 7

MHC-I and HLA-A2 expression were increased following transient LTN1 transfection of HCT116 cells. HCT116 cells were transfected with either an LTN1 or a control empty vector (EV) and the effect on panMHC class I (a) and HLA-A2 (b) expression was determined by flow cytometry. Cells transfected with HCT116 show a clear upregulation in both MHC-I and HLA-A2 expression compared to those transfected with an empty vector and wildtype cells. Data shown is representative of 3 independent experiments (Supplementary Figure 2).

As a percentage of cells will not be permissible to transfection, it is important to evaluate protein expression from the fraction of cells that have been successfully transfected. The transient LTN1 vector, pCSDest_LTN1, does not contain a selection marker, therefore within the LTN1 transfected population in Figure 7, some cells will not have been successfully transfected, potentially skewing the data. To control for transfection efficiency, HCT116 were co-transfected either LTN1 or EV with enhanced green fluorescent protein (eGFP) – cells permissible to transfection should take up and express both plasmids, therefore LTN1 transfected cells can be separated from un-transfected cells through analysis of their eGFP expression. Based on eGFP expression, transfection efficiency varied between approximately 45-60%. After sorting for eGFP, LTN1 transfected HCT116 showed a slight increase in MHC-I expression compared to HCT116 transfected with EV, or WT HCT116 (Figure 8A), however this result is mimicked in the GFP negative subset (Figure 8B) and is therefore likely not an LTN1-dependent effect. Moreover, LTN1 transfected HCT116 showed no change in HLA-A2 expression. This result is likely a consequence of maintaining the same total amount of DNA transfected into each cell culture but reducing the amount of LTN1 DNA by half to accommodate the eGFP. This result is consistent with the presence of a subset of LTN1-dependent peptides that only become available for binding when functional LTN1 is

present. Given that HLA class I expression is limited by peptide availability, this would account for the increased HLA I expression in the presence of LTN1.

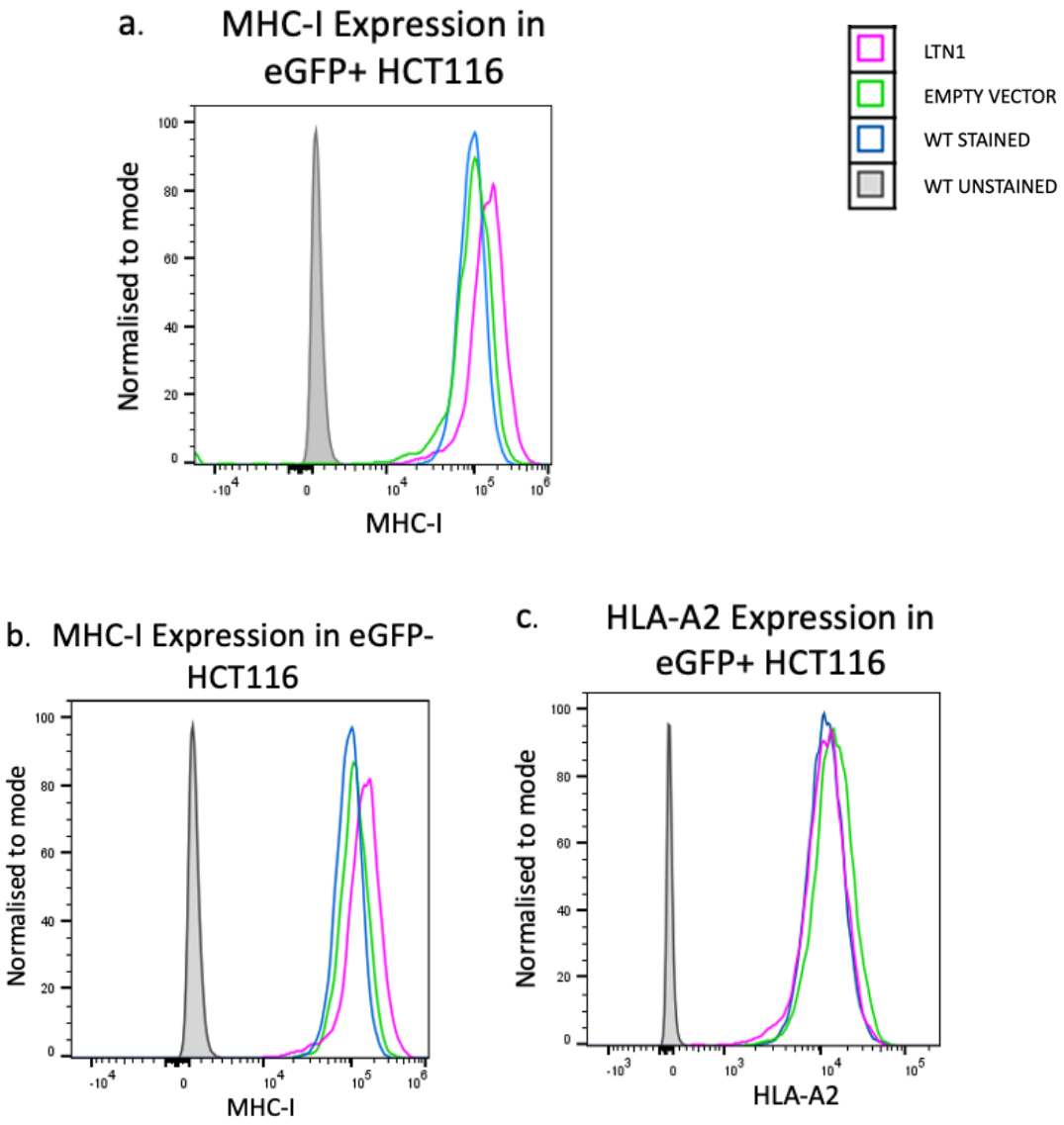


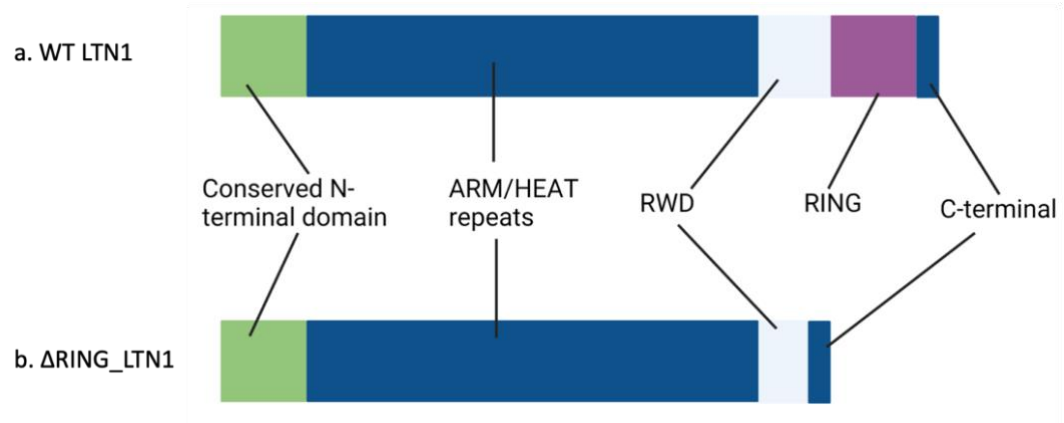
Figure 8

eGFP transiently co-transfected with LTN1 abrogated an increase in MHC-I expression.

(a) MHC-I expression of cells co-transfected with eGFP and either LTN1 or EV. (b) MHC-I expression of GFP negative subset of cells. (c) HLA-A2 expression of HCT116 co-transfected with eGFP and either LTN1 or EV. The transfection efficiency as calculated by eGFP expression is approximately 45%. Data shown is representative of 3 independent experiments.

Generation of a LTN1 RING deletion mutant

An alternative reason for the LTN1-dependent upregulation of HLA class I could be that in overexpressing LTN1, we might simply be increasing peptide supply to the classical HLA pathway, if LTN1 itself is a substrate for HLA-binding peptides. To rule this out, we attempted to generate a mutant version of LTN1 which would behave as a substrate for proteasomal degradation and consequent presentation but would not be able to function as an E3 ligase in RQC. Previous study into LTN1 activity have revealed its catalytic activity is facilitated via the RING domain[109]. In the analysis of LTN1 function in yeast, Bengston and Joazeiro (2010) studied a yeast strain in which the endogenous LTN1 lacked the catalytic RING domain[109]. This mutant form of LTN1 was found to possess no catalytic activity, leaving the protein functionally inactive, yet still able to bind the 60S ribosomal subunit, facilitated by its intact N-terminal domain. Based on this finding, it was decided in the present study to excise the RING domain from the LTN1 lentiviral vector. Both Sanger and Oxford Nanopore sequencing subsequently confirmed successful deletion of the RING domain with no off-target effects.



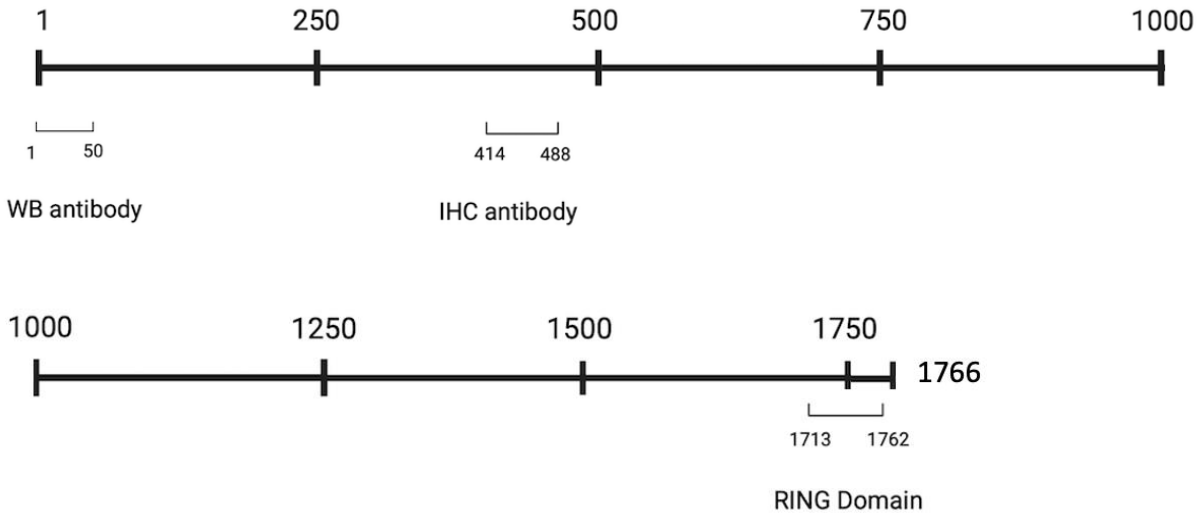


Figure 9.

Schematic diagram showing the structure of WT LTN1 and the ΔRING_LTN1 mutant.

The WT LTN1 protein (a) contains a conserved N-terminal domain, followed by 15 ARM/HEAT repeats, a RWD, RING domain, and C-terminal domain. As catalytic activity is derived from the RING domain, this was excised to generate the ΔRING_LTN1 lentiviral vector (b). (c) LTN1 amino acid sequence highlighting the binding of western blot (WB) and flow cytometry (Immunohistochemistry, IHC) antibodies, in addition to the RING domain.

To confirm the transfectability of HCT116 cells using with both the WT_LTN1 and ΔRING _LTN1 lentiviral vectors, cells were separately transiently transfected, with transfection of pCSDest LTN1 as a positive control and 48 hours post-transfection, cell lysates were collected for assessing LTN1 expression by western blot. The pCSDest_LTN1 vector served as a positive control for transfection efficiency (Figure 10). As expected, WT HCT116 cells showed no LTN1 protein expression. HCT116 cells transfected with the lentiviral LTN1 vector showed detectable bands at 201 kDa, confirming protein expression indicating that the lentiviral vector was effective in delivering the LTN1 gene into the cells and allowing for its expression. In contrast, HCT116 transfected with the ΔRING_LTN1 lentiviral vector showed

no detectable LTN1 protein expression. This finding suggests that the removal of the catalytic domain of LTN1 may result in protein instability and subsequent degradation.

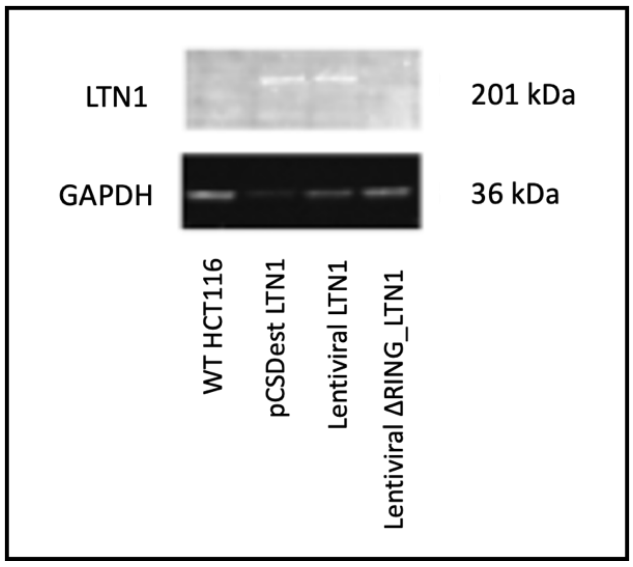


Figure 10

Western blot analysis of LTN1-transfected HCT116. LTN1 expression in HCT116 transfected transiently transfected with the pCSDest_LTN1, lentiviral LTN1 vector, and the lentiviral ΔRING_LTN1 was assessed by western blot 48 hours post transfection. LTN1 expression was detected in cells transfected with wildtype LTN1, but not ΔRING_LTN1. Wildtype untransfected HCT116 cells served as negative control.

To better understand the observed lack of LTN1 expression using the ΔRING_ LTN1 lentiviral vector, an alternative approach was utilised. An LTN1 antibody targeting a different epitope in LTN1 protein was used to perform intracellular staining and assess protein expression by flow cytometry. Specifically, the antibody used for flow cytometry detects the LTN1 amino acid sequence spanning 414 to 488, whilst the antibody used for western blot detects amino acids 1 through 50. To this end, HCT116 cells were transfected with pCSDest_LTN1, and a different preparation of the LTN1 ΔRING vector to that used in Figure

10. Figure 11 shows the resulting LTN1 expression from each experiment: HCT116 transfected with LTN1 show a significant increase in LTN1 expression compared to WT HCT116 (with geometric means of 3082 vs 735, respectively). HCT116 transfected with ΔRING_LTN1 shows a broader expression distribution of LTN1 expression (geometric mean of 2595) compared to WT.

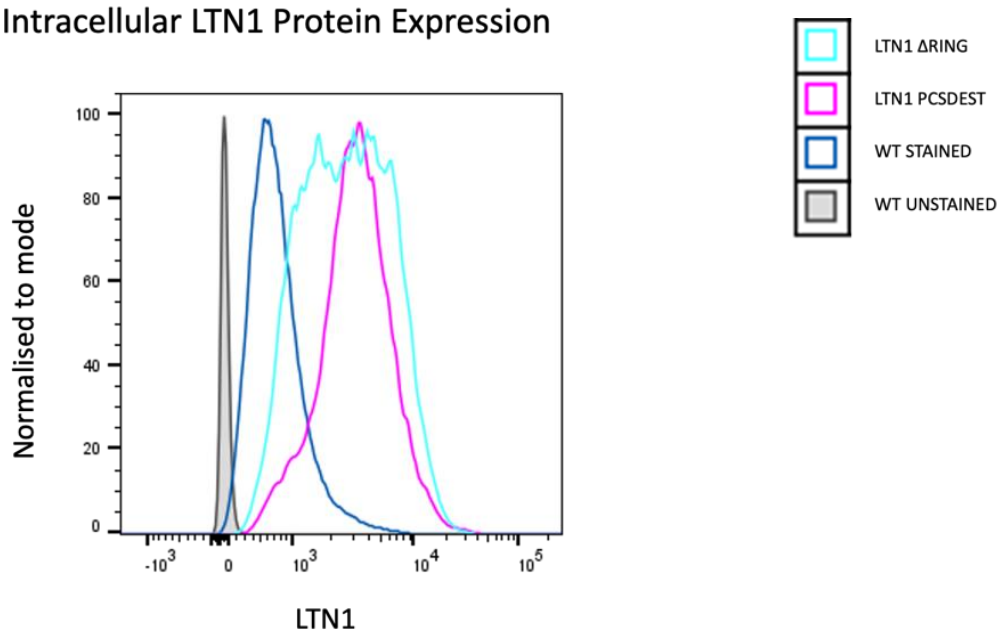


Figure 11

LTN1 expression was increased in HCT116 cells after transient transfection with ΔRING_LTN1. HCT116 cells transfected transiently with the WT_LTN1 and ΔRING_LTN1 lentiviral vectors showed an increase in LTN1 expression as detected by flow cytometry 48 hours post-transfection. N=1

After the observation that the WT_LTN1 and ΔRING_LTN1 lentiviral vectors were able to transiently transfect HCT116, it was concluded both vectors would be used for the stable transduction ofLTN1 stable. A lentiviral vector with the same backbone but lacking the LTN1

gene (termed stuffer) was used to ensure LTN1 specificity of any observed changes. Prior to lentiviral transduction, HCT116 cells were cultured with increasing concentrations of Blasticidin over a culture period of one week in order to determine the optimal concentration for selecting HCT116 cells that have been successfully transduced and carry the Blasticidin resistance gene. 8 ng/ml was identified as the optimal concentration as it demonstrated the highest percentage of dead cells at the lowest antibiotic concentration over a seven-day culture period.

To establish the LTN1 expressing HCT116 cell line, it was necessary to first package the LTN1 lentivirus. HEK293 T cells were transfected with either the stuffer or LTN1 lentiviral vector alongside second generation lentiviral packaging plasmids. 48 hours post transfection, the HEK293 lentiviral supernatant was harvested and introduced into the HCT116 cell culture. HCT116 were incubated in lentiviral supernatant for 48 hours, after which the supernatant was replenished with fresh medium for 24 hours, and Blasticidin selection commenced. The resulting cell population after 25 days of antibiotic selection were subject to western blot analysis and negative for LTN1 expression (Supplementary Figure 6). Consequently, the stable transduction procedure was repeated with modification to enhance lentiviral titre.

A potential explanation for the challenges experienced in establishing the stable expressing cell lines could be a consequence of the large size of the LTN1 gene. The LTN1 vector used is approximately 12,722 base pairs in length, extending the total size of the lentiviral vector above the upper limit for efficient transduction. The stable transduction was repeated with modifications aimed at increasing lentiviral titre. Following HEK293 T cell packaging of the LTN1 lentiviral vector, the supernatant was concentrated, and polybrene was added during

spin infection to neutralise charge repulsion between the HCT116 cell surface and lentiviral particles. As a positive control for the experimental procedure, HCT116 cells were additionally transduced following the same experimental procedure with an eGFP lentiviral vector, providing an easily visualisable marker for transduction efficiency. Seven-days post transduction, eGFP transduced HCT116 were visualised in an immunofluorescence microscope (Figure 12).

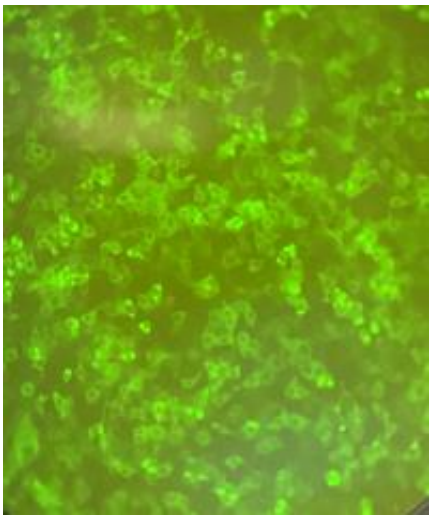


Figure 12

HCT116 cells transduced with an eGFP lentivector demonstrated high transduction efficiency. HCT116 cells were transduced with lentiviral eGFP and visualised using immunofluorescent microscopy. eGFP was expressed at a high level, serving as a positive control for the stable transduction procedure.

Twenty-five days post antibiotic selection, the WT_LTN1 transduced HCT116 cells were profiled for LTN1 expression by western blot and expression was found to be below the detection limit. To investigate whether any changes in LTN1 expression could be detected using a different antibody against LTN1 recognising a different epitope of the protein, the

transduced HCT116 were analysed by intracellular flow cytometry which failed to reveal any significant changes in LTN1 expression (Figure 13). Findings from both approaches suggest that the resistant cell clones were not able to stably express the LTN1 protein.

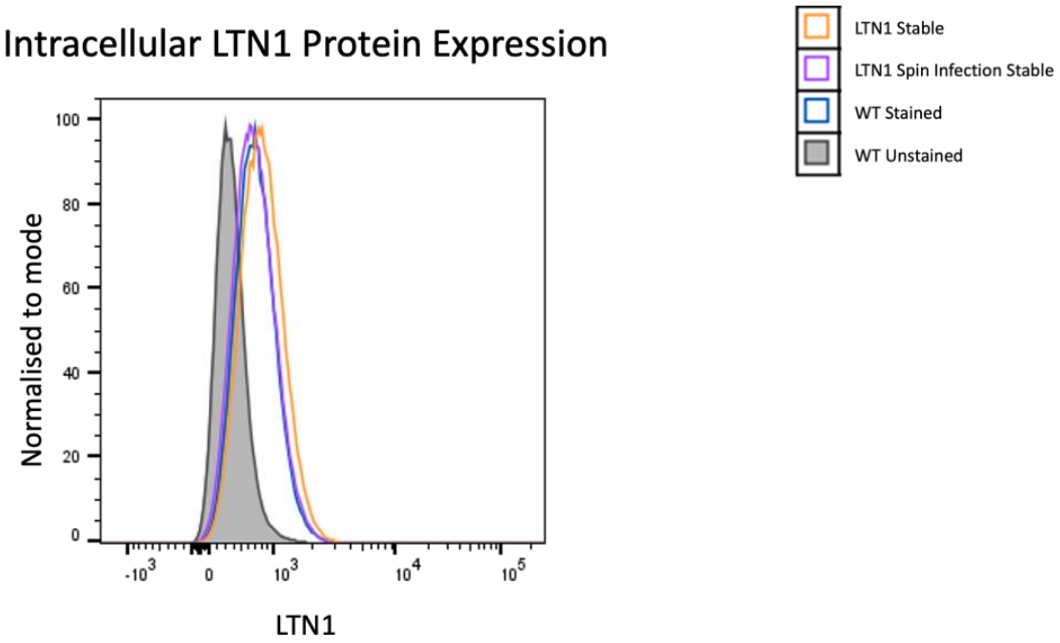


Figure 13

Blasticidin resistant cell clones do not stably express LTN1. Flow cytometric analysis of HCT116 cells following stable transduction with a LTN1 lentiviral vector showed no increase in LTN1 protein expression after 25 days of blasticidin selection. N=1

To depict the level at which LTN1 protein expression was failing in the stable cell lines, qPCR was performed to investigate the expression levels of LTN1 mRNA. Compared to WT HCT116, LTN1 transduced HCT116 showed a 5.9X increase in LTN1 mRNA (Figure 6B). This increase was also observed when comparing LTN1 transduced HCT116 to HCT116 transduced with the stuffer, only to a lesser extent (2.5X). This result suggests there is a problem with LTN1 expression on the protein level – either by degradation or detection.

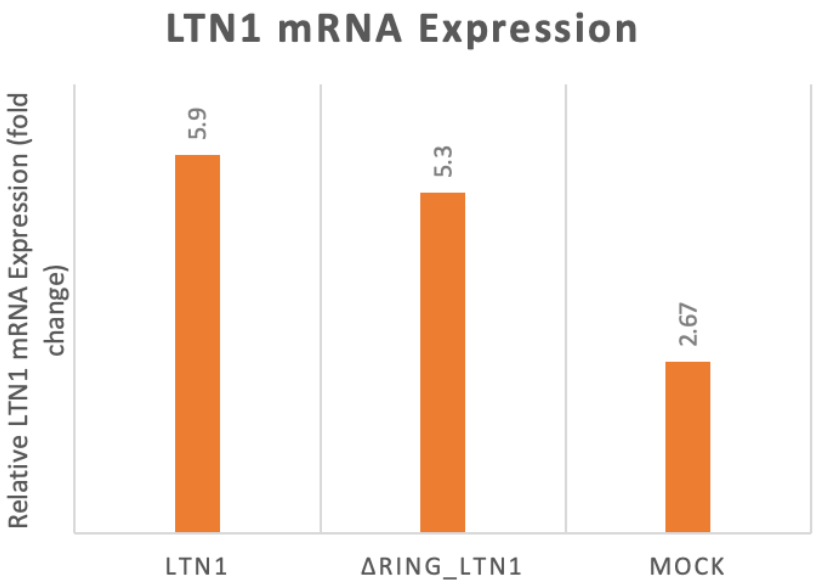


Figure 14

LTN1 mRNA expression level was increased in HCT116 cells after stable transduction with either WT_LTN1 and ΔRING_LTN1. Following Blasticidin selection, the LTN1 mRNA expression of lentiviral transduced cells was assessed by RT-qPCR analysis. Relative gene expression was calculated using the 2-ΔΔCt method, using GAPDH mRNA expression as a reference gene and wild type as the calibrator. N=2

Discussion

The selection of a biologically relevant cell line model is a crucial aspect of successful experimental design. Different tumour cell lines express different proteins, and consequently their immunopeptidomes will be distinct[110]. In order to understand the role of LTN1 specifically in MSI-H CRC, it is vital that an appropriate cell line model is used. We first surveyed the literature of LTN1 expression in CRC cell lines to aid our model selection. We then tested 10 different CRC cell lines for LTN1 genotype, mRNA expression, and protein expression as well as MHC-I expression status. Importantly, our results mimicked that observed in the literature, and a good correlation was observed between LTN1 mRNA and protein expression. HCT116 was identified as having low/no LTN1 protein expression and

genomic analysis revealed this cell line carries the same compound heterozygous mutant observed in CRC MSI patients, therefore we believe HCT116 cells to be an optimal model for translatable research. Moreover, the experimental design necessitated the chosen cell line to express MHC- I so the effect of LTN1 on the immunopeptidome could be observed. It is well established that MSI-H cancers can avoid immune detection through the mutation of HLA class I or β2-microglobulin, thus losing their cell surface expression and preventing CD8+ T cell-mediated killing[108] As the focus of the current study is to assess the impact of LTN1 loss on the global immunopeptidome of MSI CRC tumours, it was vital to select a model cell line with sufficient MHC-I expression.

Interestingly, Figure 6 demonstrates that wildtype HCT116 do express LTN1 mRNA at a low level, suggesting that this protein is being made and rapidly degraded. mRNA containing a premature stop codon, as seen in HCT116 LTN1 mRNA, is targeted by nonsense-mediated mRNA decay (NMD). The initiation of NMD can take various formats, of particular importance is the presence of an mRNA stop codon during ribosomal translation without interaction of the poly(A) tail with the poly(A) binding protein[115] This prevents proper translation termination and recruits the NMD machinery. Resultantly, the defective mRNA is degraded, however a truncated, defective polypeptide is produced. This is believed to be additionally targeted for degradation by the NDM machinery[112]. Consequently, we believe that in HCT116, NMD is targeting the defective LTN1 mRNA for degradation, and small amount of mutant LTN1 protein is rapidly degraded.

To investigate whether LTN1 can regulate MHC-I expression, HCT116 were transiently transfected with LTN1. Given that Trentini et al. showed that LTN1 enhances the expression of 103 peptides derived from 100 proteins in HeLa cells[81] our aim was to ascertain whether

these findings held true within the context of our CRC cell line model, and whether these changes translated into measurable increases in MHC- I expression. Specifically, Trentini et al. identified that these peptides were derived from hydrophobic regions within multipass transmembrane proteins[81]. Hydrophobic peptides have previously been shown to be favourably presented by HLA-A2[113], therefore we reasoned that any increase in MHC- I expression resulting from LTN1 transfection should be additionally observed in HLA-A2. An increase in both MHC-I and HLA-A2 was observed on the surface of HCT116 cells following LTN1 transfection compared to those transfected with a control empty vector (Figure 7, Supplementary Figures 2 and 3). This agrees with our hypothesis that mutations to the LTN1 gene reduce the presentation of peptide bound MHC-I. However, LTN1 is a large protein of 1766 amino acids[100] and its transient expression may introduce an increased pool of potential peptides that the cell can present on its surface thereby explaining the MHC-I upregulation. Consequently, comparing the total amount of MHC-I presented after transient LTN1 transfection may not be an accurate indicator of LTN1 functionality. One way to address this would be to transfect HCT116 with the ΔRING_LTN1 lentiviral vector and observe whether this demonstrates an increase in MHC-I expression. If ΔRING_LTN1 increases cell surface MHC-I, it is likely the observed result is a consequence of increasing peptide supply to the cell. Due to technical limitations associated with the machinery used for present flow cytometry experiments, it is vital for future work to repeat this experiment on a single flow cytometer to enable the direct statistical analysis of whether this increase in LTN1 expression is significant.

It is notable that the LTN1 vector used lacks a selection marker (i.e eGFP) for monitoring transfection efficiency. To validate protein expression using our transfection protocol, cell lysates from transiently transfected cells were analysed by western blot for LTN1 expression

and demonstrated high LTN1 expression (Supplementary Figure 1). However, it is important to recognize that transfection efficiency itself cannot be accurately inferred from total protein expression measured by western blot. In order to account for transfection efficiency, LTN1 and eGFP were co-transfected into HCT116, with eGFP serving as a selection marker, under the assumption that cells susceptible to transfection would uptake both DNA plasmids. After co-transfection of the two vectors into HCT116, flow cytometry analysis observed no change in MHC-I expression in comparison to cells that had been co-transfected with eGFP and EV (Figure 8), a finding inconsistent with Figure 7. This suggests there is not an observable increase in MHC-I expression after LTN1 transduction and the result observed in Figure 7 may be a consequence of biological variability. This diminished effect may, however, be a consequence of transfecting a lower volume of LTN1 DNA – during the co-transfection process, the total amount of DNA remained constant as in Figure 2 (2 μg) but was split between LTN1 and eGFP. Future work should test this through the transient transfection of HCT116 with just 1 μg of LTN1 to control for the lower concentration. Furthermore, future experiments should include a sample of HCT116 cells treated only with eGFP to discern any possible eGFP-related effects on MHC-I expression. Moreover, intracellular flow cytometry against LTN1 could be performed and correlated with MHC-I expression.

Future experimental work should ensure a FLAG-tag is be added to each LTN1 vector used. A FLAG-tag is a widely used 8 amino acid peptide with a specific sequence against which antibodies with particularly high affinity have been developed[114]. The addition of such a tag to the LTN1 sequence would allow the accurate detection of cells that have been transfected with LTN1 therefore providing a direct measure of transfection efficiency and ensuring the effect on MHC-I expression is not skewed by untransfected cells.

It is also important to note that transient transfection greatly amplifies the level of expression of the expressed protein above its physiological endogenous expression levels[115]. Consequently, any results observed may not be representative of the in vivo situation and the increase in MHC-I expression seen in Figure 7 may be a consequence of increasing LTN1 expression above physiologically relevant levels. As a consequence of genomic integration, the stable transduction of LTN1 helps ensure it is expressed at a physiologically relevant level, enhancing the accuracy of this cell line model. Furthermore, transient transfection has the namely limitation of the transfected protein being only transiently expressed – the plasmid DNA enters the cell nucleus, is transcribed and translated, but is not replicated with the genome during cell division[115]. Consequently, during the division of a transiently transfected cell, only one daughter cell will inherit the vector, resulting in its dilution within the population of cells, making it difficult to study at time points later than 48 hours post-transfection[115]. To combat this dilution effect, a lentiviral vector encoding LTN1 was designed for the stable transduction of HCT116 with LTN1. As lentiviral vectors integrate into the cell genome, each daughter cell produced during division will inherit a copy of the gene. This results in the gene being expressed at endogenous, biologically relevant levels[119].

To ensure the rigour of future immunopeptidomic analysis investigating LTN1 activity, it was necessary to develop an appropriate control for the transduction procedure. Bengston and Joazeiro, in their analysis of LTN1 function in yeast, studied a yeast strain in which endogenous LTN1 did not contain a RING domain, and whilst this LTN1 variant showed no catalytic activity they observe the protein is stable, retaining its capacity to interact with the 60S ribosomal subunit via its intact N-terminal domain[109]. Whilst human and yeast LTN1 show differences in their sequence, the protein is generally well conserved, owing to its vital ubiquitous functions throughout species[116]. Consequently, we here aim to generate a LTN1

RING deletion mutant to ensure that any differences observed in the immunopeptidome between HCT116 cells expressing the WT-LTN1 or the ΔRING_LTN1 are specific to the activity of LTN1.

To initially assess the transfectability of the two lentiviral vectors in HCT116, both vectors, in addition to the vector employed in the aforementioned transient transfections, were transiently transfected into HCT116. 48 hours post-transfection, cell lysates were subject to western blot analysis to assess LTN1 expression (Figure 10). Comparable bands with a molecular weight of approximately 201 kDa were observed in cells transfected with both WT LTN1 vectors. Despite this, no band was detected from HCT116 cells transfected with the ΔRING_LTN1 vector. This suggested that the removal of the catalytic domain from LTN1 resulted in protein instability and subsequent degradation—an outcome that was inconsistent to that seen in yeast[109]. To investigate this, future work should test whether the addition of a proteasome inhibitor prevents this degradation and results in the expression of ΔRING_LTN1 as detected by western blot.

To determine whether any potential contaminants may have influenced the transfection efficiency of the ΔRING_ LTN1 lentiviral vector, the transient transfection was repeated with a different preparation of the ΔRING_LTN1 vector and assessed intracellular LTN1 expression by flow cytometry as an alternative technique to gain insight into LTN1 expression. LTN1 expression within the resulting cell population showed a broad expression distribution (Figure 11), with a population of transfectants that express the same amount of LTN1 as cells transfected with pCSDest_LTN1.

Several laboratories have investigated the function of LTN1 by introducing point mutations which disrupt the amino acid reading frame, rendering the protein inactive[113]. Consequently, as an alternative approach to generating our control stable cell line containing LTN1 lacking catalytic activity, it may be useful to introduce a point mutation into our lentiviral vector and assess whether this results in the expression of mutant LTN1 after its transient transfection into HCT116.

The observation that the transient transfection of the LTN1 lentiviral vectors resulted in detectable LTN1 protein expression in HCT116 encouraged progression to establish the stable cell line. Following lentiviral transduction and a 25-day period of antibiotic selection, the resulting population of cells did not express LTN1 protein. Consequently, the stable transduction was repeated, however with modification to increase the viral titre. Such modifications included concentrating the lentiviral supernatant after HEK293 lentiviral packaging, adding polybrene to neutralise charge repulsion between the HCT116 cell surface and lentiviral particles, and comparing spin infection with regular HCT116 infection. Cell lysates were taken at multiple time points during Blasticidin selection and were analysed by western blot, revealing no LTN1 protein detection (Supplementary Figure 6). As difficulties were experienced with this particular western blot procedure, to corroborate this result, the stable cell lines were harvested for intracellular flow cytometry targeting LTN1, and no protein was detected (Figure 13). Taken together, we conclude that LTN1 was not expressed in these cell lines.

To understand the level at which protein expression failed, qPCR analysis of the stable cell lines found LTN1 mRNA to be upregulated approximately 5-fold compared with wildtype HCT116, suggesting that the issue may lie in protein expression (Figure 14). The LTN1 gene

encodes a large protein of 1766 amino acids[100], the folding and post-translational modification of which likely imposes substantial demands on cellular resources. Consequently, this protein may exhibit increased susceptibility to misfolding and subsequent degradation pathways. To address this, the addition of a proteasome inhibitor to these cell lines will prevent protein degradation. Subsequent analysis of LTN1 protein expression in the stable cell lines will discern whether the protein is being synthesised and rapidly degraded. It is necessary for future work to compare the LTN1 mRNA expression of our stable cell lines to CRC cell lines which endogenously express LTN1, such as HT-29. This assay will provide crucial insight into the relative abundance of LTN1 mRNA across these cell lines and will help inform whether additional mechanisms are at play in degrading LTN1 mRNA in the stable cell lines. This information will help delineate the factors contributing to the failure of LTN1 protein expression in the stable cell lines.

Another potential explanation for the difficulties experienced in generating the stable LTN1 expressing cell lines is the large size of the LTN1 gene and consequently the size of the lentiviral vector. The LTN1 construct used is 12,722 base pairs in length which extends the size of the lentiviral vector above the upper limit for efficient transduction. To move forwards with this approach, the lentiviral vector must be reduced in size. One possible way of reducing vector size is through the removal of the Woodchuck Hepatitis Virus (WHV) Posttranscriptional Regulatory Element (WPRE). The WPRE is 600 base pairs in length[117] and its effectiveness as an enhancer is debated within the scientific community. The WPRE within the LTN1 lentiviral vector is flanked by restriction sites, diminishing the technical challenge of its removal. Future work aims to remove this enhancer from the LTN1 lentiviral vector.

Ballhausen et al. recently identified a mutation-induced frameshift peptide derived from LTN1 as a likely immunogenic antigen when presented on the cell surface[95]. This frameshift peptide derives from the same coding microsatellite region in LTN1 where our mutation(s) of interest lie in HCT116 cells. The group used an in-silico epitope prediction pipeline to identify immunogenic peptides, taking the prevalence of HLA alleles in a defined population into account. From this analysis, LTN1 was identified as a top candidate gene for the generation of neoepitopes. Moreover, the group investigated the immunogenicity of this LTN1-derived frameshift peptide. The prediction that LTN1-derived frameshift peptides may be presented in a high percentage of MSI-H CRC patients asks whether LTN1-derived neoantigens could be potential targets in immunotherapeutic approaches. While these findings are promising, the ultimate validation necessitates data obtained from human tumour samples to ascertain whether LTN1-derived frameshift peptides are indeed presented in CRC MSI tumour cells.

Consequently, we aimed to validate this discovery in the HCT116 cell line and extend the investigation to include 20 patient-derived CRC samples, among which 4 have been classified as MSI-H. Immunopeptidomic analysis of the HCT116 cell line identified one LTN1 derived peptide, located upstream of the frameshift mutation. Specifically, this peptide is AETLSSWEA, located at position 461-469. Identification of this peptide is in line with our hypothesis that the frameshift mutation within LTN1 introduces an early stop codon, which produces a truncated protein that is rapidly degraded. The frameshift peptide identified by Ballhausen[95] however, is not detected in the HCT116 immunopeptidome. Furthermore, of the 20 clinical CRC samples, the identified LTN1 frameshift peptide was not identified in the immunopeptidome. Moving forwards, higher resolution and sensitivity mass spectrometry will be performed on these samples to obtain a deeper inspection of the immunopeptidome.

Consequently, frameshift peptides derived from LTN1 may be a candidate for preventative cancer vaccines. Vaccines, especially in comparison to conventional cancer treatments, are well tolerated and generally have a good safety profile, therefore investigating LTN1 in this context is vital for future research. In order to evaluate frameshift peptides derived from the LTN1 protein for peptide vaccines, it is vital to understand LTN1 mutation frequency and peptide expression in healthy tissue.

Mass spectrometry based immunopeptidomic analysis is a powerful technique that provides detailed insight into the peptides presented on a cell surface, thus informing ligands against which a CD8+ T cell response could be mounted[118]. Despite this, there are limitations in that low abundance peptides may not be detected as a consequence of the immunopeptidomic detection threshold, resulting loss of biologically relevant information[118]. CD8+ T cells have both the specificity and sensitivity to discriminate very low numbers of peptide presented on the cell surface[10], therefore immunopeptidomic analysis may not provide a complete picture.

Concluding remarks

This study aims to understand the involvement of LTN1 in dMMR CRC, and whilst the impact of LTN1 on the immunopeptidome remains unknown, the following study provides the foundation to answer key questions in the field. It is vital that future work utilises these results to continue the development of the stable cell line. Examining the immunopeptidome of this cell line will be necessary to provide a more complete understanding of the role of LTN1 in antigen presentation within human dMMR CRCs. Such an understanding will be vital in understanding immune evasion mechanisms in CRC and has the potential to better inform immunotherapy approaches.

Acknowledgements

I would firstly like to acknowledge my supervisory team, E. Adamopolou, T. Elliott and D. Church for their invaluable advice, support and mentorship throughout this project. I am grateful to both the University of Oxford Department of Oncology, as well as the Centre for of Immuno-Oncology for providing access to the facilities and resources that have made this research possible. I extend thanks to L. Gneo D. Arcia-Anaya, D. Lau, S. Brackenridge and R. Faure whose expertise have been instrumental in this work. Lastly, this research would not have been possible without the funding of R. and D. Smith, to whom I express my deepest gratitude.

Bibliography

1. Worldwide cancer statistics. *Cancer Research UK* https://www.cancerresearchuk.org/health-professional/cancer-statistics/worldwide-cancer (2015).

2. Knudson, A. G. Mutation and cancer: statistical study of retinoblastoma. *Proc Natl Acad Sci U S A* **68**, 820–823 (1971).

3. Hanahan, D. & Weinberg, R. A. The hallmarks of cancer. *Cell* **100**, 57–70 (2000).

4. Hanahan, D., & Weinberg, R. A. Hallmarks of cancer: the next generation - PubMed. https://pubmed.ncbi.nlm.nih.gov/21376230/.

5. Townsend, A. R. *et al.* The epitopes of influenza nucleoprotein recognized by cytotoxic T lymphocytes can be defined with short synthetic peptides. *Cell* **44**, 959–968 (1986).

6. Bassani-Sternberg, M., Pletscher-Frankild, S., Jensen, L. J., & Mann, M. (2015). Mass spectrometry of human leukocyte antigen class I peptidomes reveals strong effects of protein abundance and turnover on antigen presentation. Molecular & Cellular Proteomics, 14(3), 658-673.

7. Zinkernagel, R. M. & Doherty, P. C. Immunological surveillance against altered self components by sensitised T lymphocytes in lymphocytic choriomeningitis. *Nature* **251**, 547–548 (1974).

8. Katz, D. H. & Benacerraf, B. The regulatory influence of activated T cells on B cell responses to antigen. *Adv Immunol* **15**, 1–94 (1972).

9. Davis, M. M. & Bjorkman, P. J. T-cell antigen receptor genes and T-cell recognition. *Nature* **334**, 395–402 (1988).

10. Charles A Janeway, J., Travers, P., Walport, M. & Shlomchik, M. J. The Immune System in Health and Disease. in *Immunobiology: The Immune System in Health and Disease. 5th edition* (Garland Science, 2001).

11. Schatz, D. G. & Ji, Y. Recombination centres and the orchestration of V(D)J recombination. *Nat Rev Immunol* **11**, 251–263 (2011).

12. Hogquist, K. A., Baldwin, T. A. & Jameson, S. C. Central tolerance: learning self-control in the thymus. *Nat Rev Immunol* **5**, 772–782 (2005).

13. Abramson, J. & Anderson, G. Thymic Epithelial Cells. *Annu Rev Immunol* **35**, 85–118 (2017).

14. Hosokawa, H. & Rothenberg, E. V. How transcription factors drive choice of the T cell fate. *Nat Rev Immunol* **21**, 162–176 (2021).

15. Moran, A. E. *et al.* T cell receptor signal strength in Treg and iNKT cell development demonstrated by a novel fluorescent reporter mouse. *J Exp Med* **208**, 1279–1289 (2011).

16. Legoux, F. P. *et al.* CD4+ T Cell Tolerance to Tissue-Restricted Self Antigens Is Mediated by Antigen-Specific Regulatory T Cells Rather Than Deletion. *Immunity* **43**, 896–908 (2015).

17. Malhotra D, Linehan JL, Dileepan T, Lee YJ, Purtha WE, Lu JV et al. Tolerance is established in polyclonal CD4(+) T cells by distinct mechanisms, according to self-peptide expression patterns. Nat Immunol 2016; 17: 187–195.

18. Fontenot, J. D., Gavin, M. A. & Rudensky, A. Y. Foxp3 programs the development and function of CD4+CD25+ regulatory T cells. *Nat Immunol* **4**, 330–336 (2003).

19. Ashby, K. M. & Hogquist, K. A. A guide to thymic selection of T cells. *Nat Rev Immunol* **24**, 103–117 (2024).

20. Pellicci, D. G., Koay, H.-F. & Berzins, S. P. Thymic development of unconventional T cells: how NKT cells, MAIT cells and γδ T cells emerge. *Nat Rev Immunol* **20**, 756–770 (2020).

21. Matsushita, H. *et al.* Cancer exome analysis reveals a T-cell-dependent mechanism of cancer immunoediting. *Nature* **482**, 400–404 (2012).

22. Wu, T. & Dai, Y. Tumor microenvironment and therapeutic response. *Cancer Lett* **387**, 61–68 (2017).

23. Shang, B., Liu, Y., Jiang, S. & Liu, Y. Prognostic value of tumor-infiltrating FoxP3+ regulatory T cells in cancers: a systematic review and meta-analysis. *Sci Rep* **5**, 15179 (2015).

24. Takahashi, T. *et al.* Immunologic self-tolerance maintained by CD25+CD4+ naturally anergic and suppressive T cells: induction of autoimmune disease by breaking their anergic/suppressive state. *Int Immunol* **10**, 1969–1980 (1998).

25. Thornton, A. M. & Shevach, E. M. CD4+CD25+ immunoregulatory T cells suppress polyclonal T cell activation in vitro by inhibiting interleukin 2 production. *J Exp Med* **188**, 287–296 (1998).

26. Wing, K. *et al.* CTLA-4 control over Foxp3+ regulatory T cell function. *Science* **322**, 271–275 (2008).

27. Perez, V. L. *et al.* Induction of peripheral T cell tolerance in vivo requires CTLA-4 engagement. *Immunity* **6**, 411–417 (1997).

28. Jarnicki, A. G., Lysaght, J., Todryk, S. & Mills, K. H. G. Suppression of antitumor immunity by IL-10 and TGF-beta-producing T cells infiltrating the growing tumor: influence of tumor environment on the induction of CD4+ and CD8+ regulatory T cells. *J Immunol* **177**, 896–904 (2006).

29. Collison, L. W. *et al.* The inhibitory cytokine IL-35 contributes to regulatory T-cell function. *Nature* **450**, 566–569 (2007).

30. Turnis, M. E. *et al.* Interleukin-35 Limits Anti-Tumor Immunity. *Immunity* **44**, 316–329 (2016).

31. Biffi, G. & Tuveson, D. A. Deciphering cancer fibroblasts. J. Exp. Med. 215, 2967–2968 (2018).

32. Pancione, M. *et al.* Immune Escape Mechanisms in Colorectal Cancer Pathogenesis and Liver Metastasis. *J Immunol Res* **2014**, 686879 (2014).

33. Freeman, G. J. *et al.* Engagement of the PD-1 immunoinhibitory receptor by a novel B7 family member leads to negative regulation of lymphocyte activation. *J Exp Med* **192**, 1027–1034 (2000).

34. Wu, X. *et al.* Application of PD-1 Blockade in Cancer Immunotherapy. *Comput Struct Biotechnol J* **17**, 661–674 (2019).

35. Freeman, G. J. *et al.* Engagement of the PD-1 immunoinhibitory receptor by a novel B7 family member leads to negative regulation of lymphocyte activation. *J Exp Med* **192**, 1027–1034 (2000).

36. Dong, H., Zhu, G., Tamada, K. & Chen, L. B7-H1, a third member of the B7 family, co-stimulates T-cell proliferation and interleukin-10 secretion. *Nat Med* **5**, 1365–1369 (1999).

37. Greenwald, R. J., Freeman, G. J. & Sharpe, A. H. The B7 family revisited. Annu. Rev. Immunol. **23**, 515–548 (2005).

38. Le, D.T. et al. PD-1 blockade in tumors with mismatch-repair deficiency. N Engl J Med. **372**, 2509–2520 (2015).

39. Echols, H., & Goodman, M. F. Fidelity mechanisms in DNA replication. Annual review of biochemistry. **60**, 477–511 (1991).

40. Bębenek, A. & Ziuzia-Graczyk, I. Fidelity of DNA replication—a matter of proofreading. *Curr Genet* **64**, 985–996 (2018).

41. Kunkel, T. A. & Erie, D. A. DNA mismatch repair. *Annu Rev Biochem* **74**, 681–710 (2005).

42. Lee, J.-B. *et al.* Single-molecule views of MutS on mismatched DNA. *DNA Repair (Amst)* **20**, 82–93 (2014).

43. Jiricny, J. The multifaceted mismatch-repair system. *Nat Rev Mol Cell Biol* **7**, 335–346 (2006).

44. Kadyrov, F. A., Dzantiev, L., Constantin, N. & Modrich, P. Endonucleolytic function of MutLalpha in human mismatch repair. *Cell* **126**, 297–308 (2006).

45. Longley, M. J., Pierce, A. J. & Modrich, P. DNA polymerase delta is required for human mismatch repair in vitro. *J Biol Chem* **272**, 10917–10921 (1997).

46. Li, G. M. The role of mismatch repair in DNA damage-induced apoptosis. *Oncol Res* **11**, 393–400 (1999).

47. Huang, R. & Zhou, P.-K. DNA damage repair: historical perspectives, mechanistic pathways and clinical translation for targeted cancer therapy. *Signal Transduct Target Ther* **6**, 254 (2021).

48. Fishel, R. *et al.* The human mutator gene homolog MSH2 and its association with hereditary nonpolyposis colon cancer. *Cell* **75**, 1027–1038 (1993).

49. Nicolaides NC, Papadopoulos N, Liu B, et al. Mutations of two PMS homologues in hereditary nonpolyposis colon cancer. Nature. **371**, 75–80 (1994).

50. Fang, M., Ou, J., Hutchinson, L. & Green, M. R. The BRAF oncoprotein functions through the transcriptional repressor MAFG to mediate the CpG Island Methylator phenotype. *Mol Cell* **55**, 904–915 (2014).

51. Weisenberger, D.J., et al. CpG Island Methylator Phenotype Underlies Sporadic Microsatellite Instability and is Tightly Associated With BRAF Mutation in Colorectal Cancer. Nat Genet. **38**(7), 787–93 (2006).

52. Hause, R. J., Pritchard, C. C., Shendure, J. & Salipante, S. J. Classification and characterization of microsatellite instability across 18 cancer types. *Nat Med* **22**, 1342–1350 (2016).

53. Loeb, L. A. Human cancers express mutator phenotypes: origin, consequences and targeting. *Nat Rev Cancer* **11**, 450–457 (2011).

54. Garrido-Ramos M. A. Satellite DNA: An Evolving Topic. Genes. **8**(9), 230 (2017).

55. Boland, C.R., A National Cancer Institute Workshop on Microsatellite Instability for cancer detection and familial predisposition: Development of international criteria for the determination of microsatellite instability in colorectal cancer. Cancer Res. **58**, 5248-5257 (1998).

56. Pietrantonio, F. *et al.* Predictive role of microsatellite instability for PD-1 blockade in patients with advanced gastric cancer: a meta-analysis of randomized clinical trials. *ESMO Open* **6**, 100036 (2021).

57. Motta, R. *et al.* Immunotherapy in microsatellite instability metastatic colorectal cancer: Current status and future perspectives. *J Clin Transl Res* **7**, 511–522 (2021).

58. Saeterdal I, Bjorheim J, Lislerud K, et al. Frameshift-mutation-derived peptides as tumor-specific antigens in inherited and spontaneous colorectal cancer. Proc Natl Acad Sci USA. **98**(23), 13255–13260 (2001).

59. Linnebacher, M. *et al.* Frameshift peptide-derived T-cell epitopes: a source of novel tumor-specific antigens. *Int J Cancer* **93**, 6–11 (2001).

60. Diaz, L. A. *et al.* Pembrolizumab versus chemotherapy for microsatellite instability-high or mismatch repair-deficient metastatic colorectal cancer (KEYNOTE-177): final analysis of a randomised, open-label, phase 3 study. *Lancet Oncol* **23**, 659–670 (2022).

61. Grasso, C.S. Genetic Mechanisms of Immune Evasion in Colorectal Cancer. Cancer Discov. **8**(6), 730-749 (2018).

62. Liu, F. *et al.* Prevalence and Associations of Beta2-Microglobulin Mutations in MSI-H/dMMR Cancers. *Oncologist* **28**, e136–e144 (2023).

63. Neefjes, J., Jongsma, M. L., Paul, P., & Bakke, O. Towards a systems understanding of MHC class I and MHC class II antigen presentation. Nature Reviews Immunology, **11**(12), 823-836 (2011).

64. Vivier, E., Tomasello, E., Baratin, M., Walzer, T. & Ugolini, S. Functions of natural killer cells. *Nat Immunol* **9**, 503–510 (2008).

65. Colonna, M., Borsellino, G., Falco, M., Ferrara, G. B. & Strominger, J. L. HLA-C is the inhibitory ligand that determines dominant resistance to lysis by NK1- and NK2-specific natural killer cells. *Proc Natl Acad Sci U S A* **90**, 12000–12004 (1993).

66. Garrido, F., Cabrera, T. & Aptsiauri, N. “Hard” and “soft” lesions underlying the HLA class I alterations in cancer cells: Implications for immunotherapy. *International Journal of Cancer* **127**, 249–256 (2010).

67. Halama N, Braun M, Kahlert C, Spille A, Quack C, Rahbari N, et al.. Natural killer cells are scarce in colorectal carcinoma tissue despite high levels of chemokines and cytokines. Clin Cancer Res **17**(4), 678–89 (2011).

68. Esquivel, F., Yewdell, J. & Bennink, J. RMA/S cells present endogenously synthesized cytosolic proteins to class I-restricted cytotoxic T lymphocytes. *J Exp Med* **175**, 163–168 (1992).

69. Dhatchinamoorthy K, Colbert JD, Rock KL. Cancer Immune Evasion Through Loss of MHC Class I Antigen Presentation. Front Immunol. **12**, 636568. (2021).

70. K. L. Rock, A. L. Goldberg, Degradation of cell proteins and the generation of MHC class I-presented peptides. Annu. Rev. Immunol. **17**, 739–779 (1999).

71. Eisenack, T. J., & Trentini, D. B. Ending a bad start: Triggers and mechanisms of co-translational protein degradation. Frontiers in molecular biosciences, **9**, 1089825 (2023).

72. Yewdell, J. W., Anton, L. C., and Bennink, J. R. Defective ribosomal products (DRiPs): A major source of antigenic peptides for MHC class I molecules? J. Immunol. **157** (5), 1823–1826 (1996).

73. Yewdell, J.W. To DRiP or not to DRiP: Generating peptide ligands for MHC class I molecules from biosynthesized proteins. Mol. Immunol. **39**, 139–146 (2002).

74. Schubert, U. et al. Rapid degradation of a large fraction of newly synthesized proteins by proteasomes. Nature **404**. 6779, 770–774 (2000).

75. Blum JS, Wearsch PA, Cresswell P. Pathways of antigen processing. Annu Rev Immunol. **31**, 443-473 (2013).

76. Guo, H. J., Rahimi, N. & Tadi, P. Biochemistry, Ubiquitination. in *StatPearls* (StatPearls Publishing, 2024).

77. Goldstein, G. *et al.* Isolation of a polypeptide that has lymphocyte-differentiating properties and is probably represented universally in living cells. *Proc Natl Acad Sci U S A* **72**, 11–15 (1975).

78. Hershko, A., & Ciechanover, A. Mechanisms of enzyme-substrate recognition in proteolysis. Proceedings of the National Academy of Sciences of the United States of America, **77**(4), 1783-1786 (1980).

79. Hershko, A., Ciechanover, A., Heller, H., Haas, A. L., & Rose, I. A. Proposed role of ATP in protein breakdown: conjugation of protein with multiple chains of the polypeptide of ATP-dependent proteolysis. Proceedings of the National Academy of Sciences of the United States of America, **77**(4), 1783-1786 (1980).

80. Cruz Walma DA, Chen Z, Bullock AN, Yamada KM. Ubiquitin ligases: guardians of mammalian development. Nat Rev Mol Cell Biol. **23**(5), 350-367 (2022).

81. Trentini, D. B. *et al.* Role for ribosome-associated quality control in sampling proteins for MHC class I-mediated antigen presentation. *Proceedings of the National Academy of Sciences* **117**, 4099–4108 (2020).

82. Juszkiewicz, S. *et al.* ZNF598 Is a Quality Control Sensor of Collided Ribosomes. *Mol Cell* **72**, 469-481.e7 (2018).

83. Juszkiewicz, S. & Hegde, R. S. Initiation of Quality Control during Poly(A) Translation Requires Site-Specific Ribosome Ubiquitination. *Mol Cell* **65**, 743-750.e4 (2017).

84. Pisareva, V. P., Skabkin, M. A., Hellen, C. U. T., Pestova, T. V. & Pisarev, A. V. Dissociation by Pelota, Hbs1 and ABCE1 of mammalian vacant 80S ribosomes and stalled elongation complexes. *EMBO J* **30**, 1804–1817 (2011).

85. Joazeiro, C. A. P. Mechanisms and functions of ribosome-associated protein quality control. *Nat Rev Mol Cell Biol* **20**, 368–383 (2019).

86. Shao, S., Brown, A., Santhanam, B. & Hegde, R. S. Structure and Assembly Pathway of the Ribosome Quality Control Complex. *Mol Cell* **57**, 433–444 (2015).

87. Kuroha, K., Zinoviev, A., Hellen, C. U. T. & Pestova, T. V. Release of Ubiquitinated and Non-ubiquitinated Nascent Chains from Stalled Mammalian Ribosomal Complexes by ANKZF1 and Ptrh1. *Mol Cell* **72**, 286-302.e8 (2018).

88. Brandman, O. *et al.* A ribosome-bound quality control complex triggers degradation of nascent peptides and signals translation stress. *Cell* **151**, 1042–1054 (2012).

89. Kostova KK, Hickey KL, Osuna BA, et al. CAT-tailing as a fail-safe mechanism for efficient degradation of stalled nascent polypeptides. Science. **357**(6349), 414-417 (2017).

90. Sitron, C. S., and Brandman, O. CAT tails drive degradation of stalled polypeptides on and off the ribosome. Nat. Struct. Mol. Biol. **26**(6), 450–459 (2019).

91. Pradhan, A. K. *et al.* Ribosome-associated quality control mediates degradation of the premature translation termination product Orf1p of ODC antizyme mRNA. *FEBS Lett* **595**, 2015–2033 (2021).

92. Verma, R., Oania, R. S., Kolawa, N. J. & Deshaies, R. J. Cdc48/p97 promotes degradation of aberrant nascent polypeptides bound to the ribosome. *Elife* **2**, e00308 (2013).

93. Trentini, D. B. *et al.* Role for ribosome-associated quality control in sampling proteins for MHC class I-mediated antigen presentation. *Proceedings of the National Academy of Sciences* **117**, 4099–4108 (2020).

94. Vasaikar, S. *et al.* Proteogenomic Analysis of Human Colon Cancer Reveals New Therapeutic Opportunities. *Cell* **177**, 1035-1049.e19 (2019).

95. Ballhausen, A. *et al.* The shared frameshift mutation landscape of microsatellite-unstable cancers suggests immunoediting during tumor evolution. *Nat Commun* **11**, 4740 (2020).

96. Saeterdal, I. *et al.* Frameshift-mutation-derived peptides as tumor-specific antigens in inherited and spontaneous colorectal cancer. *Proc Natl Acad Sci U S A* **98**, 13255–13260 (2001).

97. Kloor, M. *et al.* A Frameshift Peptide Neoantigen-Based Vaccine for Mismatch Repair-Deficient Cancers: A Phase I/IIa Clinical Trial. *Clin Cancer Res* **26**, 4503–4510 (2020).

98. Gebert, J. *et al.* Recurrent Frameshift Neoantigen Vaccine Elicits Protective Immunity With Reduced Tumor Burden and Improved Overall Survival in a Lynch Syndrome Mouse Model. *Gastroenterology* **161**, 1288-1302.e13 (2021).

99. Lyumkis, D. *et al.* Single-particle EM reveals extensive conformational variability of the Ltn1 E3 ligase. *Proc Natl Acad Sci U S A* **110**, 1702–1707 (2013).

100. LTN1 - E3 ubiquitin-protein ligase listerin - Homo sapiens (Human) | UniProtKB | UniProt. https://www.uniprot.org/uniprotkb/O94822/entry.

101. Deshaies, R. J. & Joazeiro, C. A. P. RING domain E3 ubiquitin ligases. *Annu Rev Biochem* **78**, 399–434 (2009).

102. Doamekpor, S. K. *et al.* Structure and function of the yeast listerin (Ltn1) conserved N-terminal domain in binding to stalled 60S ribosomal subunits. *Proceedings of the National Academy of Sciences* **113**, E4151–E4160 (2016).

103. Vasaikar, S. et al. Proteogenomic Analysis of Human Colon Cancer Reveals New Therapeutic Opportunities. Cell. 177(4), 1035–1049 (2019).

104. Livak, K. J. & Schmittgen, T. D. Analysis of relative gene expression data using real-time quantitative PCR and the 2(-Delta Delta C(T)) Method. *Methods* **25**, 402–408 (2001).

105. Edie, S. *et al.* Survey of Human Chromosome 21 Gene Expression Effects on Early Development in Danio rerio. *G3 (Bethesda)* **8**, 2215–2223 (2018).

106. Villefranc, J. A., Amigo, J. & Lawson, N. D. Gateway compatible vectors for analysis of gene function in the zebrafish. *Dev Dyn* **236**, 3077–3087 (2007).

107. Nusinow, D. P. *et al.* Quantitative Proteomics of the Cancer Cell Line Encyclopedia. *Cell* **180**, 387-402.e16 (2020).

108. Grasso, C. S. *et al.* Genetic Mechanisms of Immune Evasion in Colorectal Cancer. *Cancer Discov* **8**, 730–749 (2018).

109. Bengtson, M. H. & Joazeiro, C. A. P. Role of a ribosome-associated E3 ubiquitin ligase in protein quality control. *Nature* **467**, 470–473 (2010).

110. Chong, C. *et al.* High-throughput and Sensitive Immunopeptidomics Platform Reveals Profound Interferonγ-Mediated Remodeling of the Human Leukocyte Antigen (HLA) Ligandome. *Mol Cell Proteomics* **17**, 533–548 (2018).

111. Amrani, N. *et al.* A faux 3'-UTR promotes aberrant termination and triggers nonsense-mediated mRNA decay. *Nature* **432**, 112–118 (2004).

112. Chu, V., Feng, Q., Lim, Y. & Shao, S. Selective destabilization of polypeptides synthesized from NMD-targeted transcripts. *Mol Biol Cell* **32**, ar38 (2021).

113. Bianchi, F., Textor, J. & van den Bogaart, G. Transmembrane Helices Are an Overlooked Source of Major Histocompatibility Complex Class I Epitopes. *Front Immunol* **8**, 1118 (2017).

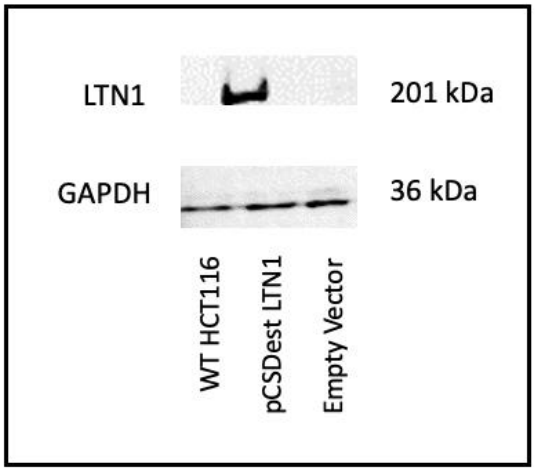
114. Hopp, T. P. *et al.* A Short Polypeptide Marker Sequence Useful for Recombinant Protein Identification and Purification. *Nat Biotechnol* **6**, 1204–1210 (1988).

115. Fus-Kujawa, A. *et al.* An Overview of Methods and Tools for Transfection of Eukaryotic Cells in vitro. *Frontiers in Bioengineering and Biotechnology* **9**, (2021).

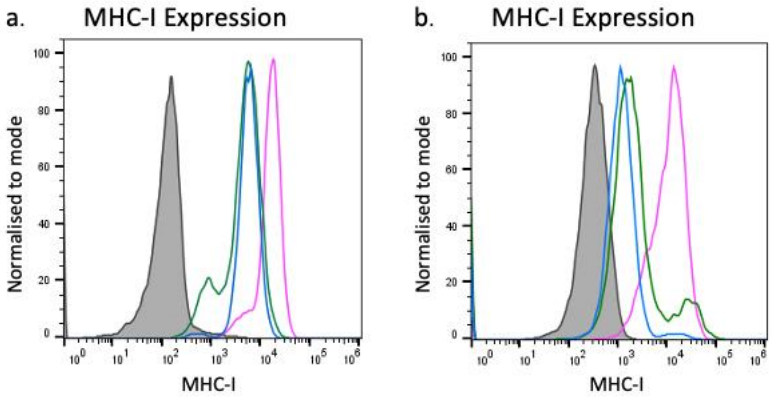
116. Joazeiro, C. A. P. Mechanisms and functions of ribosome-associated protein quality control. *Nat Rev Mol Cell Biol* **20**, 368–383 (2019).

117. Kote, S., Pirog, A., Bedran, G., Alfaro, J. & Dapic, I. Mass Spectrometry-Based Identification of MHC-Associated Peptides. *Cancers (Basel)* **12**, 535 (2020).

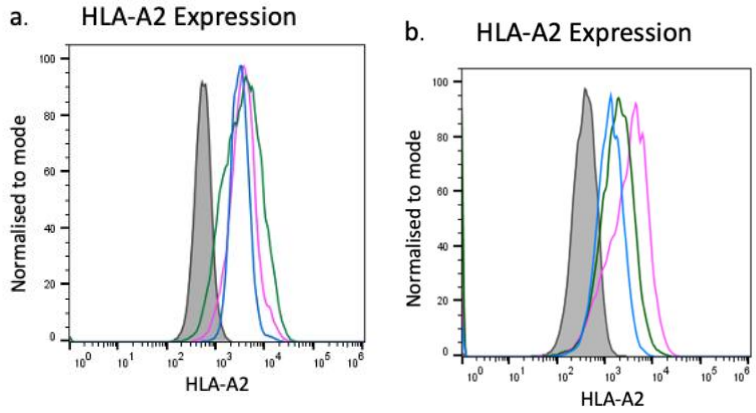
Supplementary Figures



Supplementary Figure 1
Confirmation of LTN1 transient transfection. HCT116 cells transiently transfected with LTN1 exhibited a characteristic band at 201 kDa. Wildtype HCT116 and HCT116 transfected with an empty vector did not express LTN1, as expected.

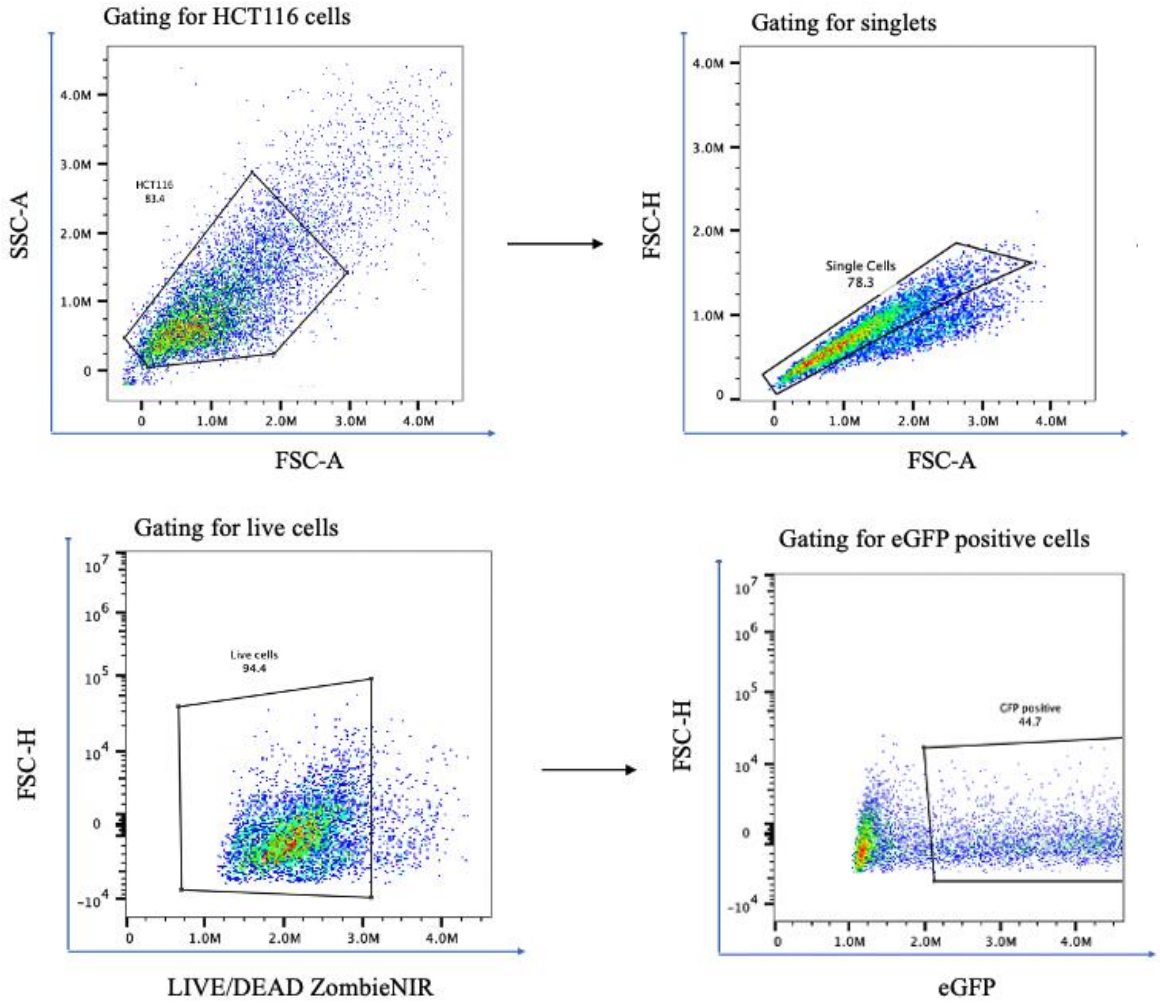


Supplementary Figure 2
Repeats of LTN1 transfection of HCT116. Due to technical limitations, these results were collected on different flow cytometry machines, preventing the direct statistical analysis of the repeats.

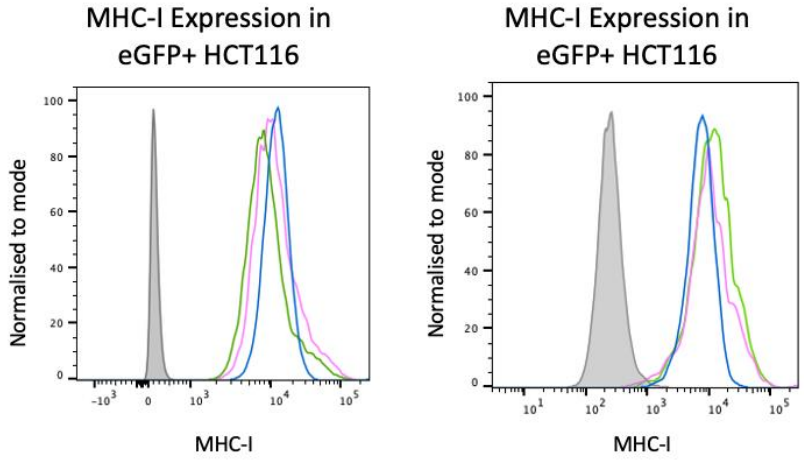


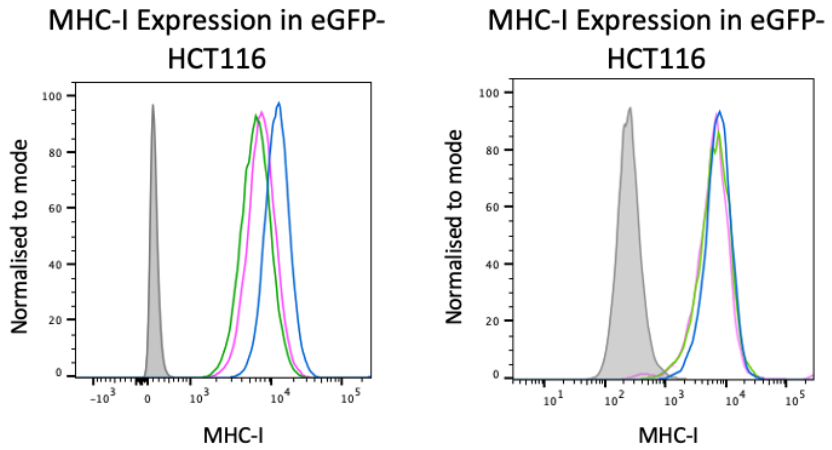
Supplementary Figure 3

Repeat experiments of LTN1 transient transfection of HCT116. Due to technical limitations, these results were collected on different flow cytometry machines, preventing the direct statistical analysis of the repeats.

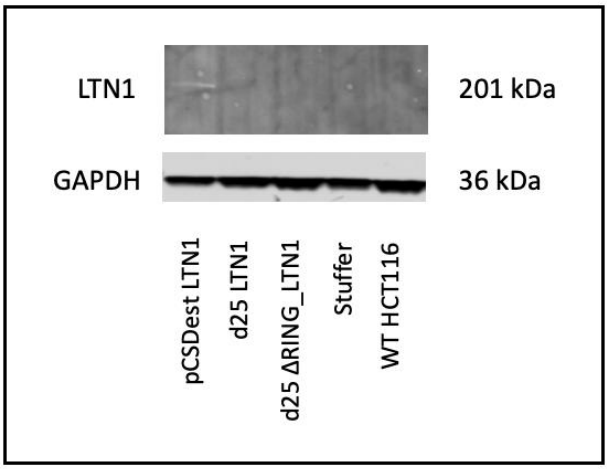


Supplementary Figure 4
Gating strategy of flow cytometry data from Figure 8. The same gating strategy was used consistently throughout all flow cytometry analysis. All flow cytometry analysis was conducted in FlowJo 10.10.0.





Supplementary Figure 5
Repeat experiments of eGFP co-transfection of HCT116 with LTN1. Transfection of HCT116 with LTN1 had no effect on MHC-I expression. Due to technical limitations, these results were collected on different flow cytometry machines, preventing the direct statistical analysis of the repeats.



Supplementary Figure 6
Western blot of HCT116 transduced with LTN1 25 days post selection. HCT116 transfected with transient LTN1 show a characteristic band at 201 kDa, albeit at low visibility due to technical limitations associated with the antibody. HCT116 cells transduced with LTN1 and ΔRING_LTN1 exhibited no LTN1 protein expression 25 days post selection, as did cells transfected with a control stuffer and wildtype HCT116.